© 2016. Published by The Company of Biologists Ltd | Development (2016) 143, 1674-1687 doi:10.1242/dev.133728

STEM CELLS AND REGENERATION

RESEARCH ARTICLE

Integrin signalling regulates YAP and TAZ to control skin homeostasis

Ahmed Elbediwy[1,*], Zoé I. Vincent-Mistiaen[1,*], Bradley Spencer-Dene[1], Richard K. Stone[1], Stefan Boeing[1], Stefanie K. Wculek[1], Julia Cordero[2], Ee H. Tan[2], Rachel Ridgway[3], Val G. Brunton[3], Erik Sahai[1], Holger Gerhardt[1], Axel Behrens[1], Ilaria Malanchi[1], Owen J. Sansom[2] and Barry J. Thompson[1,‡]

ABSTRACT

The skin is a squamous epithelium that is continuously renewed by a population of basal layer stem/progenitor cells and can heal wounds. Here, we show that the transcription regulators YAP and TAZ localise to the nucleus in the basal layer of skin and are elevated upon wound healing. Skin-specific deletion of both YAP and TAZ in adult mice slows proliferation of basal layer cells, leads to hair loss and impairs regeneration after wounding. Contact with the basal extracellular matrix and consequent integrin-Src signalling is a key determinant of the nuclear localisation of YAP/TAZ in basal layer cells and in skin tumours. Contact with the basement membrane is lost in differentiating daughter cells, where YAP and TAZ become mostly cytoplasmic. In other types of squamous epithelia and squamous cell carcinomas, a similar control mechanism is present. By contrast, columnar epithelia differentiate an apical domain that recruits CRB3, Merlin (also known as NF2), KIBRA (also known as WWC1) and SAV1 to induce Hippo signalling and retain YAP/TAZ in the cytoplasm despite contact with the basal layer extracellular matrix. When columnar epithelial tumours lose their apical domain and become invasive, YAP/TAZ becomes nuclear and tumour growth becomes sensitive to the Src inhibitor Dasatinib.

KEY WORDS: Hippo pathway, Integrin, Yes-associated protein, TAZ, Stratified squamous epithelium

INTRODUCTION

The Yes-associated protein (YAP) family of transcriptional co-activators are emerging as potent oncoproteins that strongly drive cell proliferation in many types of stem/progenitor cells and cancers (Harvey et al., 2013; Irvine and Harvey, 2015; Pan, 2010, 2015; Piccolo et al., 2013). The function of YAP family co-activators was first discovered by *Drosophila* genetics, where the sole YAP homologue Yorkie (Yki) was found to be necessary and sufficient to promote cell proliferation and tissue overgrowth in epithelia (Huang et al., 2005). Subsequent genetic experiments in mice showed that ectopic expression of YAP (also known as YAP1) was sufficient to drive cell proliferation in liver, intestine, bronchus and skin (Cai et al., 2010; Camargo et al., 2007; Dong et al., 2007; Schlegelmilch et al., 2011; Zhang et al., 2011a; Zhao et al., 2014). Surprisingly, YAP knockout mice have mild phenotypes, although they are deficient in proliferative repair of the intestine and resistant to intestinal tumour formation (Azzolin et al., 2014; Cai et al., 2010), as well as showing reduced bronchial stem cells (Zhao et al., 2014) and kidney defects (Reginensi et al., 2015). An important and widespread physiological role for YAP in mice might be obscured by the possibility of redundancy between YAP and TAZ (also known as WWTR1) a second mammalian family member that is highly similar in both sequence and function.

At the molecular level, Yki and YAP were shown to function by associating with the DNA-binding transcription factor Scalloped (Sd; or TEAD in humans) to drive transcription of anti-apoptotic and pro-proliferative target genes (Koontz et al., 2013; Liu-Chittenden et al., 2012; Vassilev et al., 2001; Wu et al., 2008). Other co-factors of Yki/YAP that promote transcription include WBP2 (Zhang et al., 2011b), MASK1/2 (Sansores-Garcia et al., 2013; Sidor et al., 2013) and the SWI/SNF complex (Jin et al., 2013; Oh et al., 2013). The activity of Yki was found to be regulated by the *Drosophila* Hippo-Warts (Hpo-Wts) kinase signalling pathway, in which Wts directly phosphorylates Yki to promote its relocalisation from the nucleus to the cytoplasm (Dong et al., 2007; Huang et al., 2005; Oh and Irvine, 2008). In human cells in culture, YAP nuclear localisation is similarly inhibited upon LATS1/2 kinase phosphorylation, because phosphorylated YAP is retained the cytoplasm by binding to 14-3-3 family proteins (Dong et al., 2007; Zhao et al., 2007). This entire molecular system is now referred to as the Hippo signalling pathway.

Much recent work has aimed to identify upstream regulators of Hippo signalling. A group of apically localised proteins including Crumbs (Crb, CRB1/2/3 in humans), Merlin (Mer, NF2 in humans), Expanded (Ex, similar to Willin and AMOT in humans) and Kibra (Kib, KIBRA or WWC1 in humans) were found to activate Hippo signalling (repressing Yki activity) in *Drosophila* epithelia (Baumgartner et al., 2010; Chen et al., 2010; Genevet et al., 2010; Hamaratoglu et al., 2006; Ling et al., 2010; Varelas et al., 2010; Yu et al., 2010) and in mice (Szymaniak et al., 2015). In addition, a group of adherens junction-localised proteins including Ajuba (Jub), Zyxin (Zyx), Dachs, Mib and Riquiqui (Riq), were shown to inhibit Hippo signalling (activating Yki) in *Drosophila* epithelia (Cho et al., 2006; Das Thakur et al., 2010; Degoutin et al., 2013; Gaspar et al., 2015; Mao et al., 2006; Rauskolb et al., 2011). Finally, manipulation of the level of F-actin in *Drosophila* can also affect Hippo signalling, possibly via signalling through the Src kinase, which can promote Yki activation (Enomoto and Igaki, 2013; Fernandez et al., 2011, 2014; Sansores-Garcia et al., 2011). Human YAP and TAZ were subsequently found to act as F-actin responsive mechanosensors in cell culture (Aragona et al., 2013; Benham-Pyle et al., 2015; Dupont et al., 2011; Zhao et al., 2007),

[1]The Francis Crick Institute, 44 Lincoln's Inn Fields, London WC2A 3LY, UK. [2]The Beatson Institute, Switchback Rd, Bearsden, Glasgow G61 1BD, UK. [3]Edinburgh Cancer Research Centre, University of Edinburgh, Western General Hospital, Crewe Road South, Edinburgh EH4 2XR, UK.
*These authors contributed equally to this work

[‡]Author for correspondence (barry.thompson@crick.ac.uk)

Received 3 December 2015; Accepted 9 March 2016

Development (2016) 143, 1674-1687 doi:10.1242/dev.133728

but how their subcellular localisation is physiologically regulated in human epithelial tissues and cancers *in vivo* remains a fundamental unsolved problem.

Here, we examine the physiological function and regulation of YAP and TAZ in mammalian epithelial tissues. We focus on stratified squamous epithelia, particularly the skin, and compare our findings with columnar epithelia, such as the intestine and bronchus. We propose that YAP and TAZ act as sensors of both apical and basal signals *in vivo*, and that this regulatory logic explains why these proteins localise to the nucleus in basal stem/progenitor cells to promote cell proliferation and tissue renewal. Elevation of YAP and TAZ can then drive increased cell proliferation during wound healing or tumour formation.

RESULTS

YAP and TAZ are expressed in both mouse and human skin, and regulate gene expression in basal layer stem/progenitor cells

We began by characterising the expression and subcellular localisation of YAP and TAZ in both mouse and human skin. Both proteins were found to be expressed and nuclear localised in a subset of cells in the skin of the mouse embryo, neonate and adult. Nuclear localisation of YAP and TAZ was particularly prominent in basal layer cells of both interfollicular epidermis and the hair follicle (Fig. 1A). Some nuclear localisation was also detected in the highly flattened squamous cells, consistent with results in cell culture where cell flattening induces nuclear accumulation of YAP and TAZ (Dupont et al., 2011) (Fig. 1A). Human YAP and TAZ show a similar pattern of subcellular localisation in sections of adult human skin (Fig. 1B). Basal layer cells feature nuclear YAP and TAZ, whereas differentiating daughters feature cytoplasmic YAP and TAZ (Fig. 1B). Again, some nuclear localisation is also detectable in highly flattened squamous cells that have terminally differentiated (Fig. 1B).

To confirm that YAP and TAZ are transcriptionally active in the skin, we sought to identify YAP-regulated genes by an RNA-sequencing (RNA-seq) approach in human keratinocytes. mRNA was isolated from cells expressing activated mutant YAP^{5SA} or siRNAs against *YAP* and subjected to RNA-seq and gene-set enrichment analysis (Fig. 1C, Fig. S1). We found that the YAP-regulated gene sets included: the previously identified Hippo/YAP reactomes; cell cycle reactomes (such as E2F targets or cyclin E-associated genes); cell growth reactomes (such as Myc, global translation regulators or regulation of ornithine

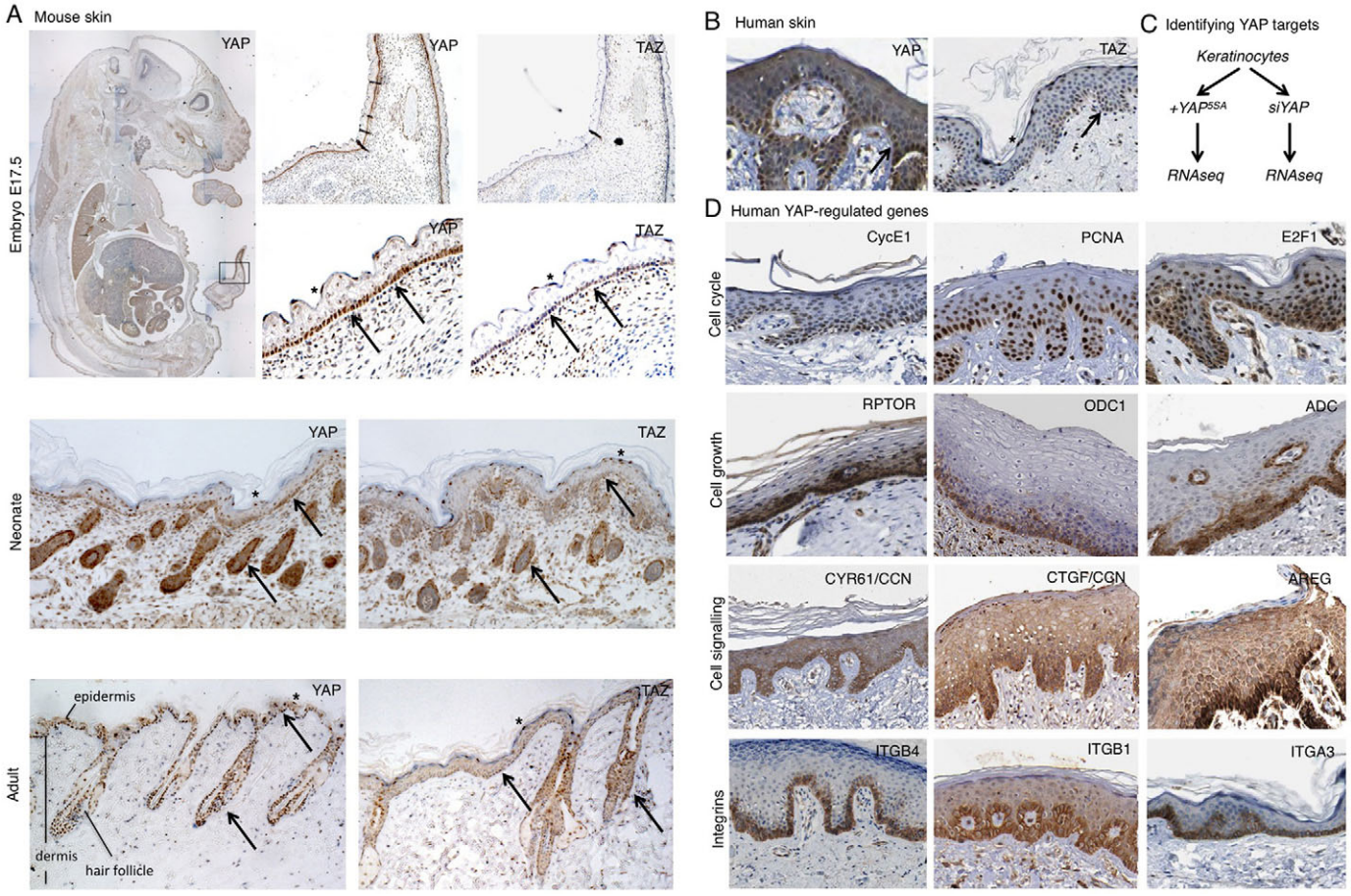

Fig. 1. YAP and TAZ are expressed in both mouse and human skin and regulate gene expression in basal layer stem cells. (A) Mouse skin at three developmental stages, including embryonic (E17.5), neonate and adult. Tissue sections were stained for either YAP or TAZ to reveal their expression and subcellular localisation. (B) Human skin (adult) stained for either YAP or TAZ. Note the nuclear localisation in basal layer stem/progenitor cells as well as terminally differentiating flattened cells. Other differentiating cells have cytoplasmic YAP and TAZ localisation. Arrows indicate nuclear YAP/TAZ; asterisks indicate flattened suprabasal cells with nuclear YAP/TAZ. (C) Analysis of YAP-dependent gene expression by RNA-seq was performed by comparison of YAP gain and loss of function in keratinocytes (see Fig. S1). (D) YAP-regulated genes identified by RNA-seq analysed for their expression patterns in skin tissue by mining the Human Protein Atlas dataset (see Materials and Methods). Strong enrichment in basal layer stem/progenitor cells is evident for many target genes, indicating that YAP and TAZ are transcriptionally active in this population of cells.

Development (2016) 143, 1674-1687 doi:10.1242/dev.133728

decarboxylase); cancer signalling reactomes (such as EGFR-Ras signalling targets); and cancer microenvironment/metastasis reactomes (including regulators of cellular interactions with the extracellular matrix) (Fig. S1). We therefore analysed the expression of the corresponding cell cycle [CycE1 (CCNE2), PCNA, E2F1], cell growth [RPTOR, ODC1, ADC (AZIN2)] and EGFR and integrin signalling (CYR61, CTGF, AREG, integrins α3, α6, β1, β2, β4) regulators (Fig. 1D). We found a striking restriction of these YAP targets to the basal layer of the skin, indicating that YAP/TAZ transcriptional regulation is active exclusively in the basal stem/progenitor cell population (Fig. 1D).

YAP and TAZ are required for skin homeostasis

To examine the physiological role of YAP and TAZ, we generated double conditional knockout (dKO) mice with the skin-specific Keratin5-CreERT recombinase. Compared with control animals, the YAP/TAZ dKO mice showed a dramatic loss of hair in patches beginning 2 weeks after tamoxifen injection in adult mice, or causing complete blockade of hair growth in neonates treated with tamoxifen (Fig. 2A,B). Histological sections of the skin revealed expression and nuclear localisation of YAP and TAZ in control skin, which was lost in the dKO tissue. Proliferation of basal layer cells, as marked by Ki67 staining, was clearly reduced in YAP/TAZ dKO skin (Fig. 2A,B), as was YAP target gene expression (Fig. S2). These phenotypes are reminiscent of skin-specific conditional knockouts of integrin β1 (ITGB1) (Brakebusch et al., 2000; Grose et al., 2002; Piwko-Czuchra et al., 2009; Raghavan et al., 2000; Singh et al., 2009).

We next tested whether YAP and TAZ contribute to skin repair after wounding. We found that levels of both YAP and TAZ were elevated after wounding, particularly in the basal cell layer of the epidermis where strong nuclear staining is visible (Fig. 2C,D). We next recorded the time taken to repair small (4 mm) wounds in the back skin of control versus YAP/TAZ dKO mice. We found that control wounds normally healed completely by 10 days, whereas dKO wounds failed to heal within 10 days and instead required an additional 2 days to heal (Fig. 2E,F). This delay in healing was not observed when YAP or TAZ were deleted individually. To investigate the cause of the delay in wound healing, we examined

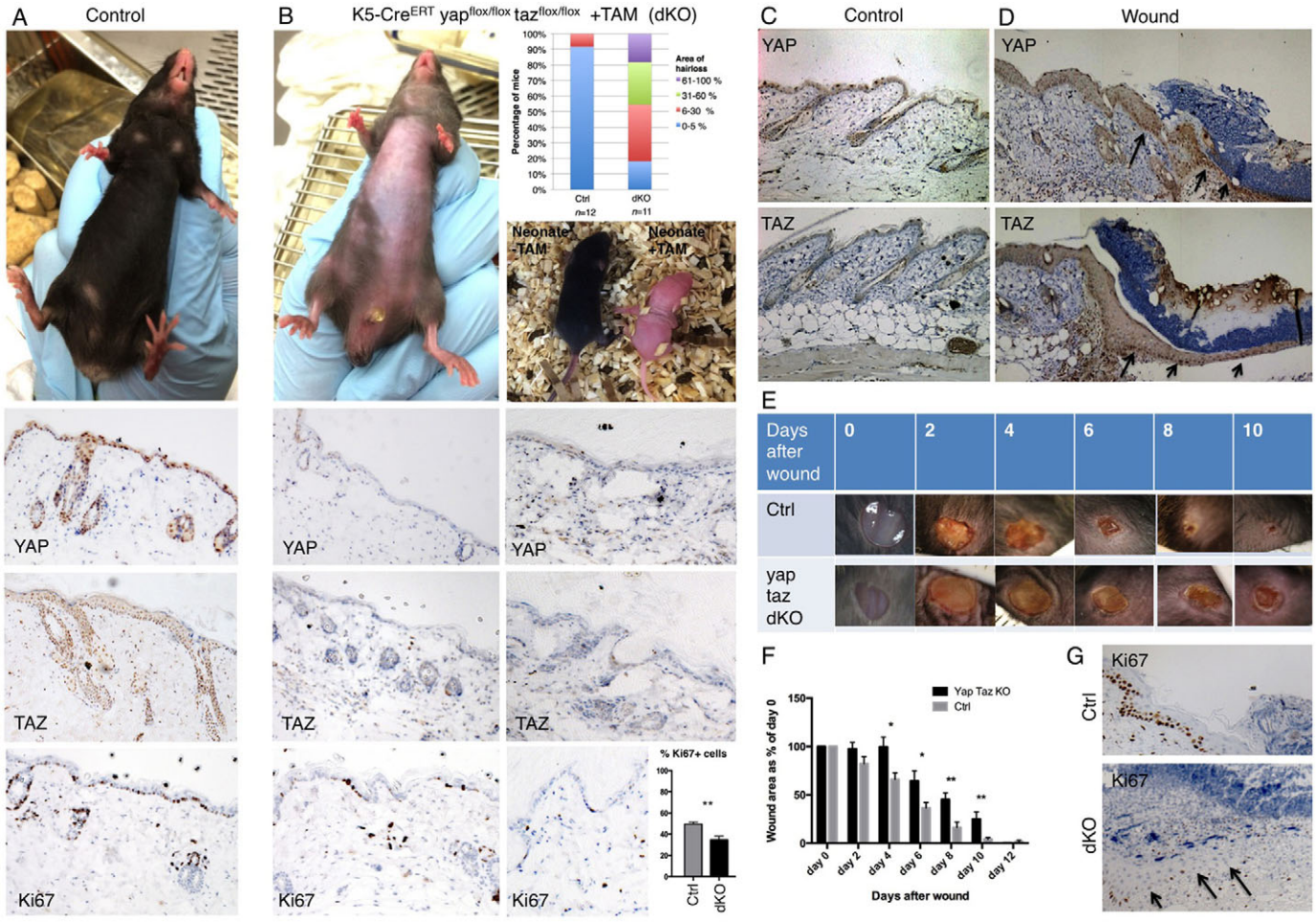

Fig. 2. Conditional inactivation of YAP and TAZ impairs skin homeostasis and wound repair in mice. (A) Control mice have a thick layer of hair (fur) covering their skin, which sections reveal is positive for YAP, TAZ and Ki67 (a marker of cell proliferation). (B) Double conditional knockout mice for YAP and TAZ treated with tamoxifen as adults or neonates exhibit dramatic hair loss. Adult skin sections are negative for YAP and TAZ, and have reduced levels of Ki67^{+} positive cells (quantified as a percentage of total interfollicular basal cells in each randomly selected 40× field of view. n=757 control cells; n=896 dKO cells). (C) Control mouse skin stained for YAP and TAZ. (D) Punch biopsy wound edge stained for YAP and TAZ. (E) Imaging of wound healing in control (n=8) and YAP/TAZ double conditional knockout mice (dKO; n=8). Note delayed healing in dKO. (F) Quantification of wound healing rates in control versus dKO animals. ImageJ was used to measure the wound area at each stage. (G) Proliferation of cells as marked by Ki67 staining is reduced in dKO wounds versus control animals. Values are means±s.e.m. *P<0.05, **P<0.01.

Development (2016) 143, 1674-1687 doi:10.1242/dev.133728

cell proliferation in wounds of control versus dKO mice. We found that the number of $Ki67^+$ cells was reduced in dKO wounds versus controls (Fig. 2G). These findings demonstrate a crucial, physiological requirement for YAP and TAZ in basal layer stem/progenitor cells to promote cell proliferation.

In the skin of the ITGB1 conditional knockout mice, cells that escape Cre-mediated recombination are able to repopulate the mutant skin in a short time frame (Piwko-Czuchra et al., 2009). We found that the same phenomenon occurs in YAP/TAZ dKO skin, where after Cre activation and YAP/TAZ deletion, either YAP^+ or TAZ^+ residual cells expanded their territory, consistent with the notion that YAP and TAZ promote proliferation of basal layer cells (Fig. S3). This phenomenon was also evident during wound healing, where YAP or TAZ positive cells were able to populate the wound and allow proliferation and healing in dKO animals (Fig. S3). These findings underscore the importance of YAP and TAZ in epidermal progenitor cell proliferation and skin homeostasis and suggest a close relationship between integrin signalling and YAP/TAZ function.

Mechanisms controlling nuclear localisation of YAP in basal layer cells

We next sought to understand how YAP and TAZ become nuclear localised in basal layer cells. Since YAP and TAZ are similar proteins that localise identically in skin, we henceforth focus on the regulation of YAP localisation. Recent work in cultured MCF10A breast cancer cells indicate a role for integrin-Src signalling and EGFR-PI3K signalling in promoting the nuclear localisation of YAP (Fan et al., 2013; Kim and Gumbiner, 2015). To test whether these pathways are active in skin, we examined their expression and subcellular localisation. By mining the Human Protein Atlas dataset, we found that ITGB1, SRC, EGFR and AKT2 (a marker of PI3K activation) are all expressed strongly in basal layer cells, with AKT2 recruited to the interface between basal layer epidermal cells and the underlying basement membrane extracellular matrix (Fig. 3A-E). This pattern is also evident in other squamous epithelia such as cervix or oesophagus and is retained in squamous cell carcinomas (Fig. 3A-E). These data suggest that nuclear YAP localisation might be stimulated by integrin-Src and/or PI3K signalling in basal layer skin keratinocytes (Fig. 3F).

To confirm that integrin-Src and PI3K signalling pathways are required for YAP nuclear localisation in keratinocytes, we systematically manipulated these pathways with siRNA knockdown or treatment with specific inhibitor compounds in human keratinocytes in culture. We found that inhibition of ITGB1 with blocking antibodies or siRNA, inhibition of the downstream effectors SRC or FAK, or inhibition of PI3K profoundly impairs

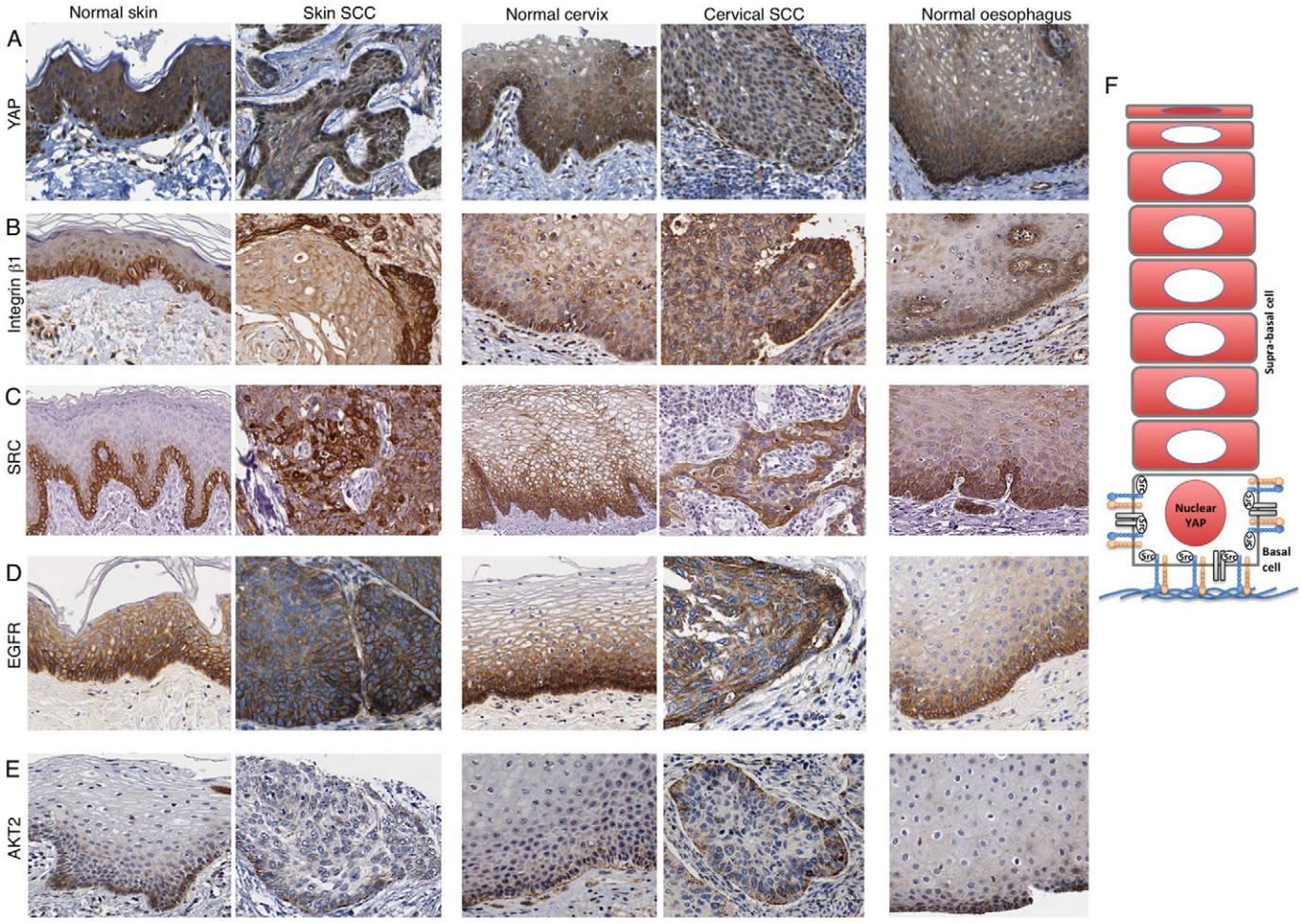

Fig. 3. Integrin-Src and EGFR-PI3K localisation in human stratified squamous epithelia and squamous cell carcinomas (SSCs). The Human Protein Atlas dataset was mined to compare the expression and localisation of potential YAP regulators in human skin sections. YAP staining reveals basal layer nuclear localisation (A), ITGB1, SRC and EGFR staining reveals basal layer expression (B-D) and AKT2 staining reveals basal subcellular localisation (E) across squamous tissue types and cancers. (F) Model for YAP regulation in stratified squamous epithelia.

Development (2016) 143, 1674-1687 doi:10.1242/dev.133728

YAP nuclear localisation (Fig. 4A,B). Interestingly, inhibition of the PI3K effectors AKT and TORC1 had no effect on YAP localisation, whereas inhibition of PDK1 did partially impair YAP nuclear localisation (Fig. 4C). Notably, drugs inhibiting F-actin, myosin II or Rho kinase had only a moderate effect on YAP localisation in keratinocytes (Fig. 4D). Quantification of these phenotypes highlights the strong effect of inhibition of integrin-Src and PI3K (Fig. 4E). Both Src inhibitors and PI3K inhibitors led to a clear increase in phosphorylated YAP (p-YAP), indicating that Hippo signalling (MST-LATS signalling) is elevated by these treatments (Fig. 4F). We confirmed these findings in a classic 'scratch-wound' assay, where Src inhibition completely reversed the nuclear localisation of YAP at the leading edge (Fig. 4G). These findings indicate that integrin-Src and EGFR-PI3K signalling are essential for YAP nuclear localisation in keratinocytes (Fig. 4H).

To extend these findings *in vivo*, we examined the role of integrin-Src signalling in mouse skin. We compared YAP localisation in untreated and TPA-treated (inflamed) skin samples from control animals and knockouts for FAK or Src (Fig. 5A-C). We found that loss of FAK or Src results in decreased YAP levels and nuclear localisation in both normal and inflamed skin (Fig. 5A-C). Some nuclear YAP remained in flattened cells (Fig. 5A-C, asterisks). Similar results were obtained by treatment of mice with the topical Src inhibitor (Dasatinib), which was able to drastically reduce YAP levels and nuclear localisation in untreated or TPA-treated skin, as well as in skin papillomas induced by a TPA +DMBA treatment regimen (Fig. 5D-I). These findings show that integrin-Src signalling is crucial to promote YAP stabilisation and nuclear localisation in basal layer stem/progenitor cells. Accordingly, recent work indicates that skin papillomas induced by DMBA+TPA in mice can be strongly reduced in size and frequency by homozygous deletion of YAP along with one copy of TAZ or by treatment with Dasatinib (Creedon and Brunton, 2012; Serrels et al., 2009; Zanconato et al., 2015).

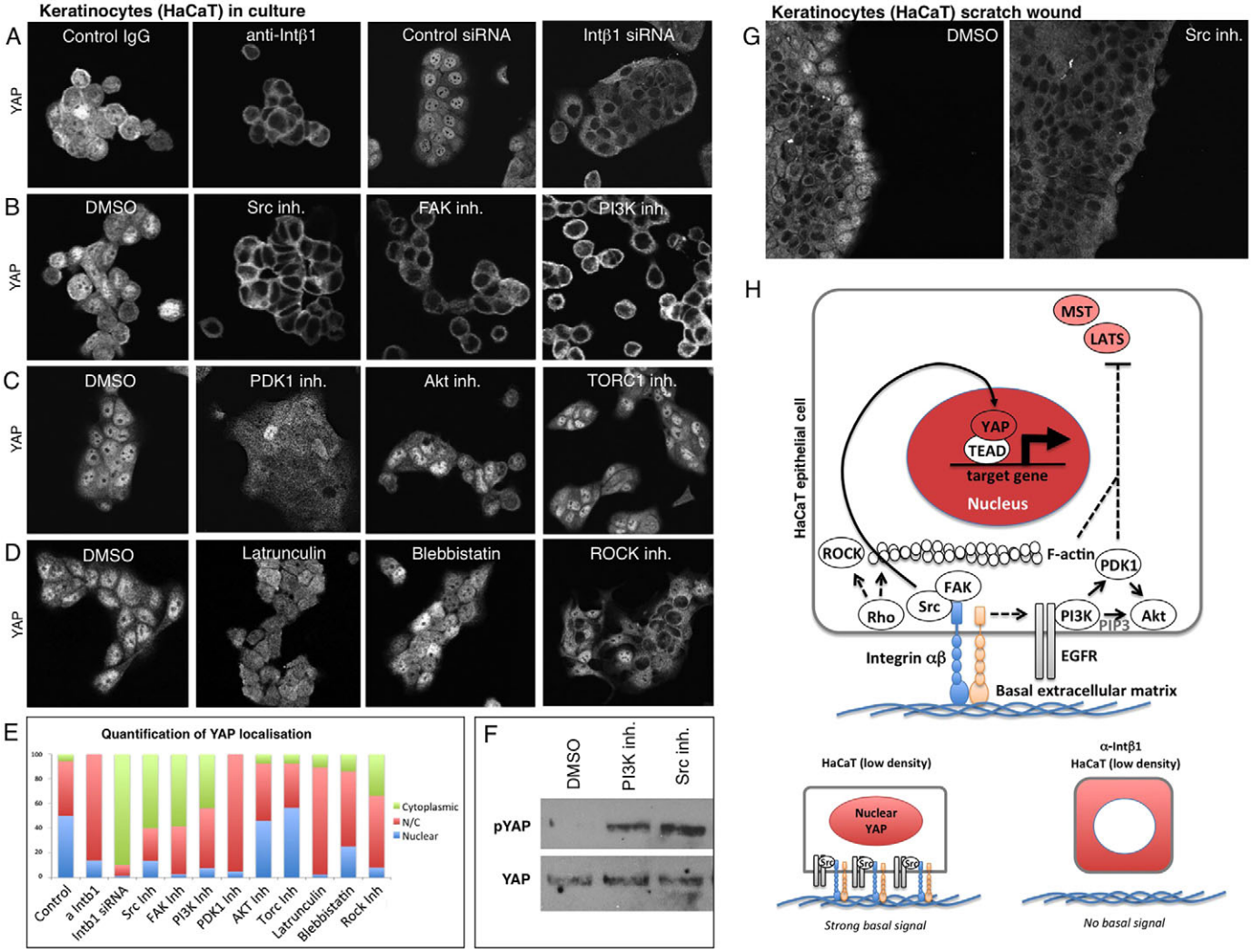

Fig. 4. Basal integrin-Src signalling promotes nuclear localisation of YAP in human HaCaT keratinocyte epithelial cells. (A) YAP nuclear localisation is prevented by treatment of keratinocytes with anti-ITGB1 antibodies (PD52) or by *ITGB1* siRNA treatment. (B) YAP nuclear localisation is prevented by treatment of keratinocytes with the Src inhibitor Dasatinib, by the FAK inhibitor PF573228 or by the PI3K inhibitor GDC0941, but not by treatment with DMSO solvent. (C) YAP nuclear localisation is reduced by treatment of keratinocytes with the PDK1 inhibitor BX795, but not by the AKT inhibitor MK2206, TORC1 inhibitor Everolimus or DMSO solvent. (D) YAP nuclear localisation is reduced by treatment of keratinocytes with the F-actin destabilising drug Latrunculin, the myosin II inhibitor Blebbistatin, or the Rho-kinase inhibitor Y27632. (E) Quantification of A-D. (F) Western blotting analysis of p-YAP levels in keratinocytes treated with either DMSO control, PI3K inhibitor or Src inhibitor. Total YAP levels are shown as a control. (G) Nuclear YAP localisation at the leading edge of a scratch wound in keratinocyte culture is abolished by treatment with the Src inhibitor Dasatinib. (H) Schematic diagram of YAP regulation in keratinocytes.

Development (2016) 143, 1674-1687 doi:10.1242/dev.133728

Mechanisms controlling YAP cytoplasmic localisation in differentiating daughter cells of squamous versus columnar epithelia

The above analysis suggests that daughter cells differentiate in the skin simply by loss of contact with the basement membrane extracellular matrix and consequent loss of integrin-Src signalling, EGFR-PI3K signalling and YAP nuclear localisation. This model is plausible in all stratified squamous epithelia, but cannot explain the self-renewal versus differentiation decision in columnar epithelia because differentiated columnar epithelial cells retain contact with the basement membrane. Thus, columnar cells must employ an additional mechanism to promote YAP localisation to the cytoplasm. An obvious candidate is the expression of a differentiated apical plasma membrane domain in columnar epithelial cells, because apical proteins associated with Crumbs (CRB3) are well known to induce Hippo signalling (MST-LATS signalling) to drive YAP to the cytoplasm (Chen et al., 2010; Fletcher et al., 2015; Ling et al., 2010; Szymaniak et al., 2015; Varelas et al., 2010).

To test this notion *in vivo*, we compared the subcellular localisation of YAP with that of CRB3 in columnar epithelia in the gallbladder, endometrium, lung bronchus, breast duct, urinary bladder, small intestine, colon and salivary gland. In all cases, apical localisation of CRB3 in differentiated daughter cells correlated with cytoplasmic localisation of YAP (Fig. 6A-H). Accordingly, basal layer stem/progenitor cells of the lung, breast or intestine retained nuclear YAP but lack apical CRB3. Notably, CRB3 is not expressed in squamous epithelia so cannot mediate the regulation of YAP in these tissues (Fig. 6I-L). The key Hippo pathway components Merlin, SAV1 and KIBRA colocalised with CRB3 (Figs S4 and S5) (Chen et al., 2010; Genevet et al., 2010; Hamaratoglu et al., 2006; Ling et al., 2010; Yin et al., 2013; Yu et al., 2010; Zhang et al., 2010). These results indicate that a universal regulatory logic exists

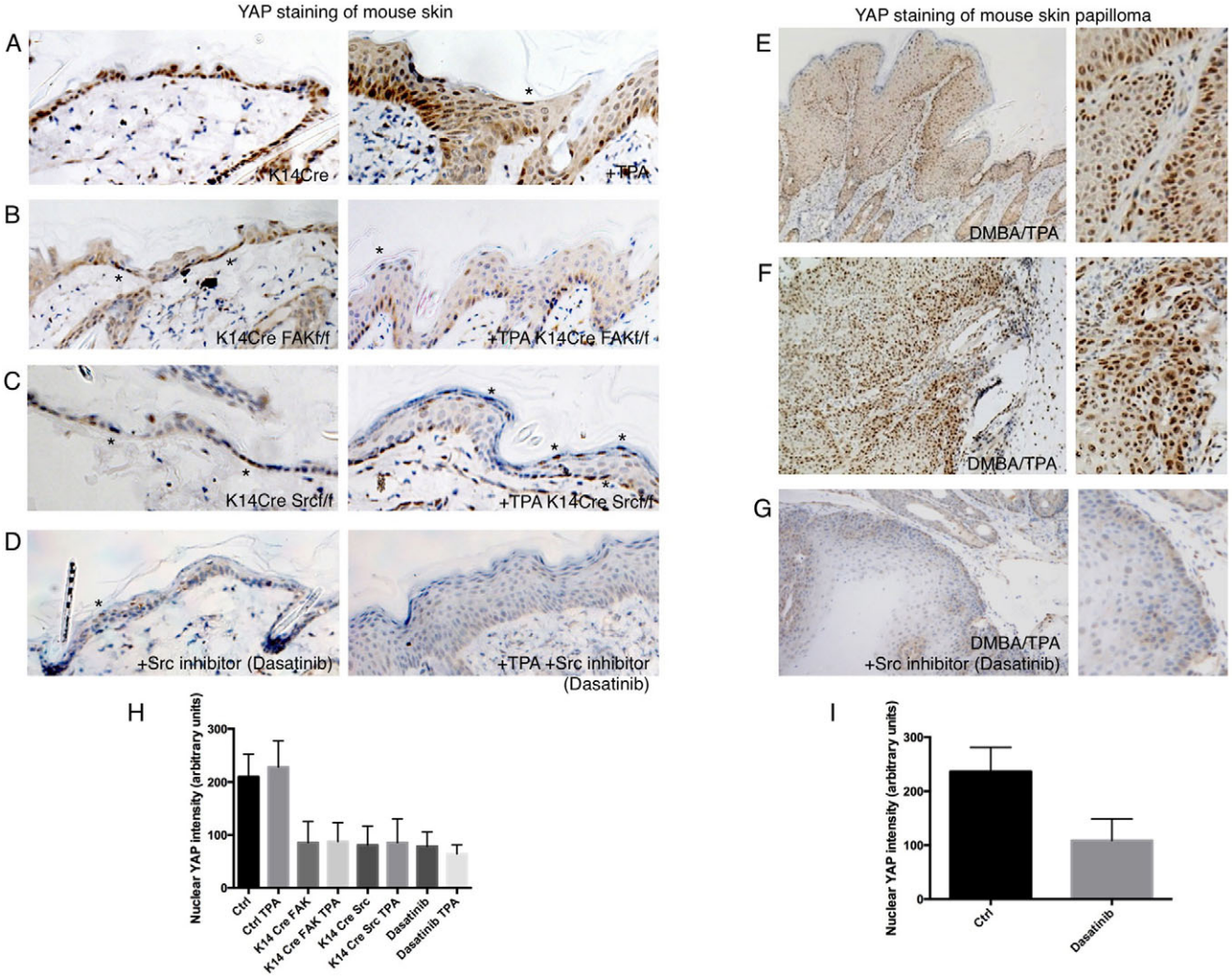

Fig. 5. Basal integrin-Src signalling promotes YAP stability and nuclear localisation in mouse skin. (A) YAP staining in control and TPA-treated skin to induce hyperplasia. (B) YAP staining is reduced in FAK conditional KO skin before or after treatment with TPA. Note some residual nuclear YAP localisation in basal layer cells or highly flattened cells (asterisk). (C) YAP staining is reduced in Src conditional KO skin before or after treatment with TPA. Note that there is some residual nuclear YAP localisation in basal layer cells or highly flattened cells (asterisks). (D) YAP staining is reduced in Dasatinib-treated skin before or after treatment with TPA for 2 days. Note there is some residual nuclear YAP localisation in basal layer cells or highly flattened cells (asterisk). (E) YAP staining of mouse skin papilloma induced by DMBA-TPA treatment of mice expressing *v-Ha-Ras* (see Materials and Methods). Note stronger nuclear localisation in the basal layer. (F) YAP staining of mouse skin squamous cell carcinoma induced by DMBA-TPA treatment of *v-Ha-Ras*-expressing mice. (G) YAP staining is strongly reduced by treatment of DMBA-TPA induced papillomas with the Src inhibitor Dasatinib topically for 3 days. (H) Quantification of nuclear YAP intensity in A-D. (I) Quantification of nuclear YAP intensity in F,G. Values are means±s.e.m.

Development (2016) 143, 1674-1687 doi:10.1242/dev.133728

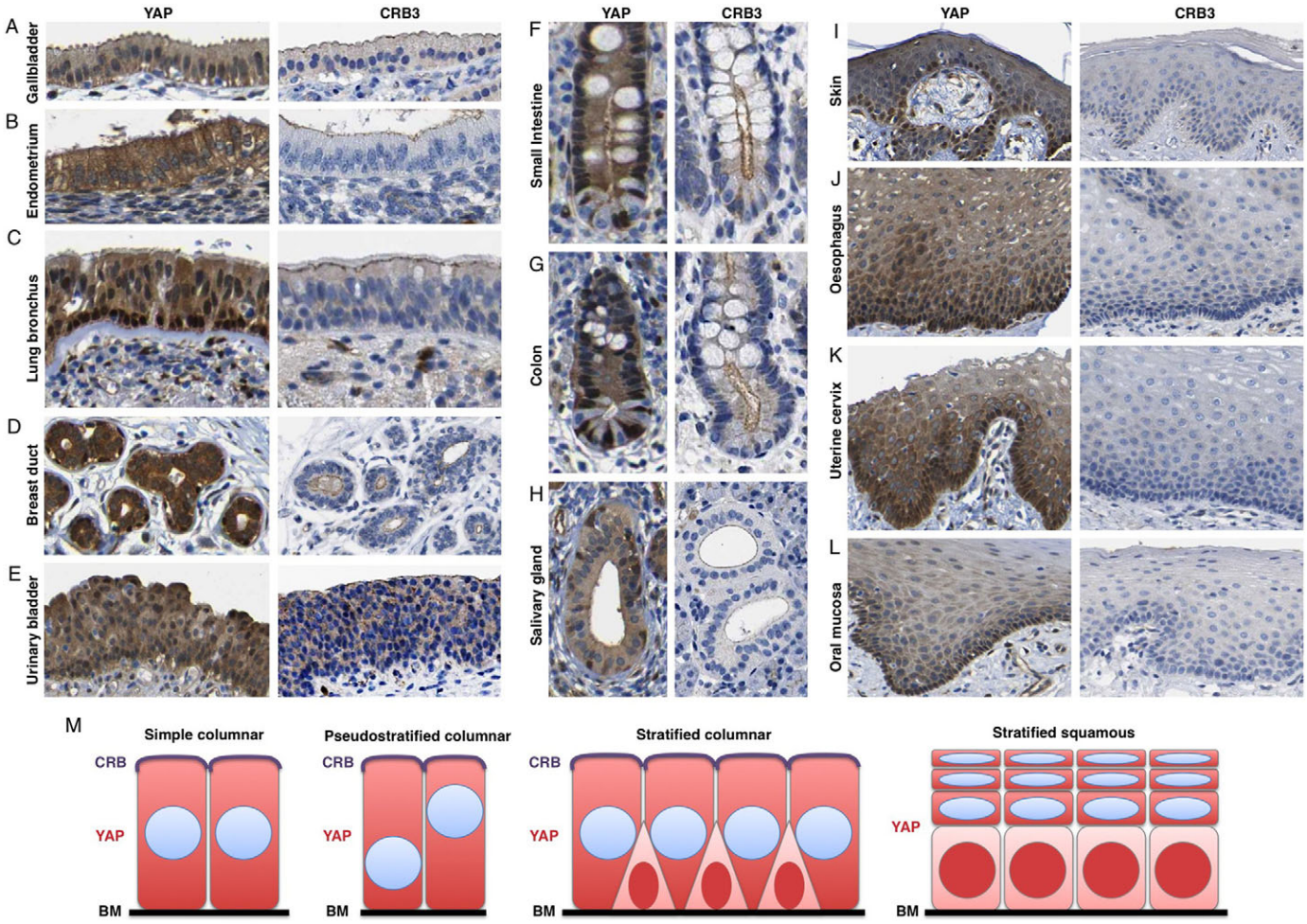

Fig. 6. Apical-domain formation inhibits YAP nuclear localisation in human columnar epithelia. The Human Protein Atlas dataset was mined to compare the localisation of YAP with the presence of absence of the apical domain in different epithelia. YAP localises to the cytoplasm in columnar gallbladder epithelium (A) and columnar endometrial epithelium (B) which have a CRB3^{+} apical domain. (C) YAP localises to the nucleus of basal layer stem/progenitors, which lack CRB3 expression, and cytoplasm in columnar epithelial cells, which have a CRB3^{+} apical domain, in the bronchus. (D) YAP localises to the nucleus of basal layer stem/progenitors, which lack CRB3 expression, and cytoplasm in columnar epithelial cells, with a CRB3^{+} apical domain, in the breast. (E) YAP localises to the cytoplasm in pseudostratified columnar bladder epithelium, with a CRB3^{+} apical domain. (F) YAP localises to the nucleus of crypt base stem/progenitors, which lack a large CRB3^{+} apical domain, and cytoplasm in columnar epithelial cells, which feature a large CRB3^{+} apical domain, in the small intestine. (G) YAP localises to the nucleus of crypt base stem/progenitors, which have a small CRB3^{+} apical domain, and cytoplasm in columnar epithelial cells, which feature a large CRB3^{+} apical domain, in the colon. (H) YAP localises to the nucleus of basal layer stem/progenitors, which lack CRB3 expression, and cytoplasm in columnar epithelial cells, which have a CRB3^{+} apical domain, in the salivary gland. (I-L) YAP localises to the nucleus of basal layer stem/progenitors, and cytoplasm of differentiating squamous epithelial cells, even though the entire tissue lacks CRB3 expression. (M) Schematic diagram of YAP localisation in different epithelial tissue types.

in which YAP nuclear localisation requires contact with the basement membrane but is inhibited by expression of an apical domain (Fig. 6M).

We next sought to confirm that apical and basal signals act antagonistically in columnar epithelial cells. We examined human intestinal epithelial cells in culture that are capable of forming 3D cysts or 2D monolayers in which YAP becomes cytoplasmic. We found that siRNA knockdown of the apical determinant CDC42 or LATS1/2 has similar effects, driving YAP to the nucleus (Fig. 7A,B). Strong YAP nuclear localisation can also be achieved simply by plating these cells at low density, so that they are unable to differentiate an apical domain and also retain a flat morphology with an extensive basal surface area (Fig. 7C). This basal contact appears to invoke the same integrin-Src signals identified in keratinocytes, because blocking of integrins with low Ca^{2+}, anti-ITGB1 antibodies or *ITGB1* siRNAs relocalised YAP to the cytoplasm (Fig. 7C). Inhibition of Src, FAK, PI3K or PDK1 also impaired YAP nuclear localisation (Fig. 7D,E). These effects are once again as strong as inhibition of F-actin, myosin II or Rho kinase (Fig. 7F,G). Examination of p-YAP levels indicated that integrin-Src signalling acts via regulation of MST-LATS phosphorylation of YAP (Fig. 7H). These results suggest that apical domain formation activates LATS kinases to retain YAP in the cytoplasm, whereas basal integrin-Src and PI3K signalling inhibits LATS kinases to promote nuclear YAP localisation (Fig. 7I).

To further explore these findings *in vivo*, we examined how YAP behaves in columnar epithelial tumours that progress to invasive adenocarcinomas. We found that YAP remains cytoplasmic whereas tumours of the colon, stomach, lung, endometrium, urothelium or ovary retained their columnar epithelial form (Fig. 8A-F). By contrast, invasive adenocarcinomas of the same

Development (2016) 143, 1674-1687 doi:10.1242/dev.133728

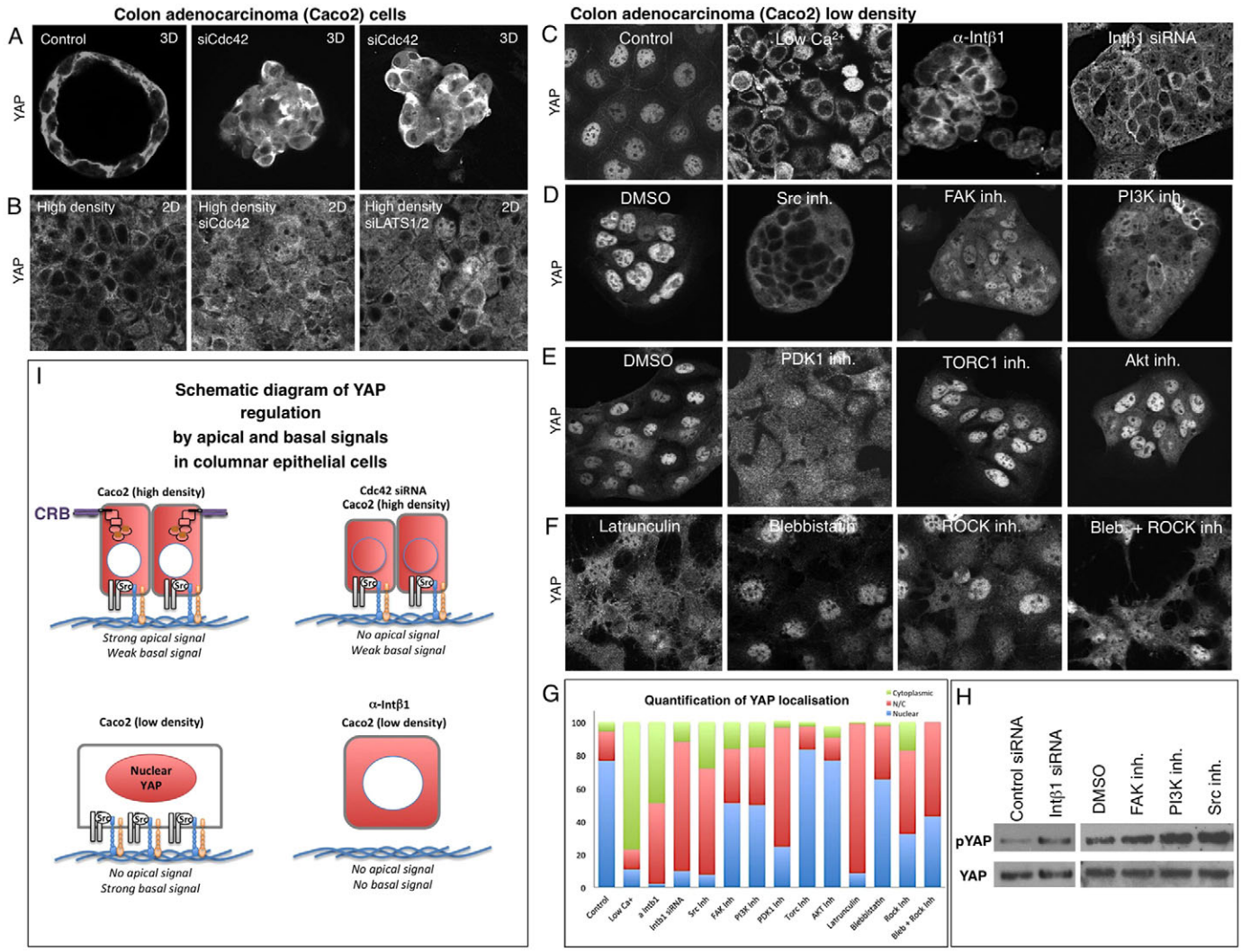

Fig. 7. Basal integrin-Src signalling promotes YAP nuclear localisation in human Caco2 epithelial cells when apical domain formation is blocked. (A) Caco2 colon adenocarcinoma cells form 3D cysts in cell culture that feature cytoplasmic YAP localisation. Silencing of *CDC42* by siRNA knockdown disrupts apical-basal polarity and induces more nuclear YAP localisation. (B) Caco2 colon adenocarcinoma cells form 2D epithelial monolayers at high density. Silencing of *CDC42* by siRNA knockdown disrupts apical-basal polarity and induces more nuclear YAP localisation, similar to silencing of *LATS1/2*. (C) YAP nuclear localisation is very strong when Caco2 cells are plated at low density to prevent apical domain formation. Nuclear localisation is prevented by treatment of Caco2 cells with low-calcium medium, anti-ITGB1 antibodies (PD52) or by *ITGB1* siRNA treatment, but not in controls. (D) YAP nuclear localisation is prevented by treatment of Caco2 cells with the Src inhibitor Dasatinib, by the FAK inhibitor PF573228 or by the PI3K inhibitor GDC0941, but not by treatment with DMSO solvent. (E) YAP nuclear localisation is reduced by treatment of Caco2 cells with the PDK1 inhibitor BX795, but not by the AKT inhibitor MK2206, TORC1 inhibitor Everolimus or DMSO solvent. (F) YAP nuclear localisation is reduced by treatment of Caco2 cells with the F-actin destabilising drug Latrunculin, the myosin II inhibitor Blebbistatin or the Rho kinase inhibitor Y27632, or a combination of Blebbistatin and Y27532. (G) Quantification of C-F. (H) Western blotting analysis of p-YAP levels in Caco2 cells treated with control siRNAs or *ITGB1* siRNAs, as well as DMSO control, FAK inhibitor, PI3K inhibitor or Src inhibitor. Total YAP levels are shown as a control. (I) Schematic diagram of YAP regulation in Caco2 cells.

tissue origin all featured a loss of columnar form and a dramatic localisation of YAP to the nucleus (Fig. 8A-F). These results suggest that loss of the apical domain during tumour progression allows YAP to become nuclear. We therefore tested whether nuclear YAP in invasive adenocarcinomas would be sensitive to inhibition of integrin-Src signalling with Dasatinib. We examined *Apc*$^{-/-}$ *p53* (*Trp53*)$^{-/-}$ mutant intestinal organoids that had been implanted subcutaneously into nude mice. On transplantation, these organoids rapidly produce highly invasive adenocarcinomas, entering the surrounding stromal tissue. We found that YAP localisation became strongly nuclear, specifically in the invasive tumour cells (Fig. 8G). We next treated mice carrying such invasive tumours with the Src inhibitor Dasatinib, which strongly suppressed nuclear YAP localisation and reduced tumour growth and invasion (Fig. 8H). These findings indicate that Src activity promotes YAP nuclear localisation *in vivo* and suggest a potential therapy for invasive adenocarcinomas and carcinomas.

DISCUSSION

Our results identify a physiological role for YAP and TAZ in skin homeostasis, promoting cell proliferation in basal layer stem/progenitor cells (Figs 1, 2). YAP and TAZ localise to the nucleus of basal layer cells to drive transcription of a set of genes associated with cell cycle progression, cell growth, EGFR signalling and cell-matrix adhesion via integrins. In the absence of YAP and TAZ, proliferation is reduced and dramatic hair loss occurs, indicating that YAP and TAZ are crucial players in the stem/progenitor cell biology of the skin. Importantly, loss of either YAP or TAZ individually had

Development (2016) 143, 1674-1687 doi:10.1242/dev.133728

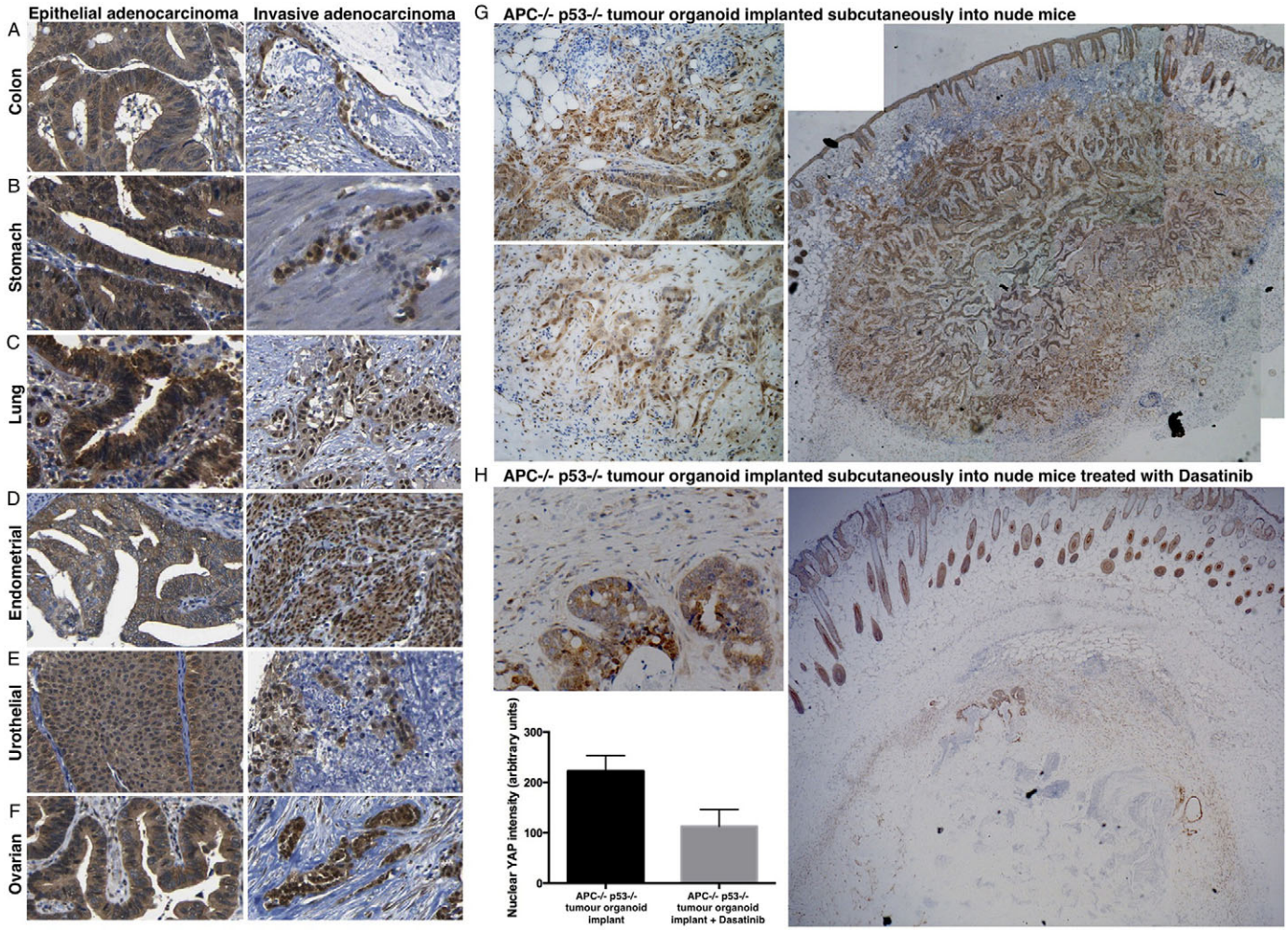

Fig. 8. YAP becomes nuclear in invasive adenocarcinomas, which become sensitive to Dasatinib. In the colon (A) and stomach (B) YAP localises to the cytoplasm of columnar epithelial cells in epithelial adenocarcinoma, and the nucleus of invasive adenocarcinoma cells, which have lost their columnar shape and lack a lumen. (C) In the bronchus, YAP localises to the nucleus of basal layer stem/progenitors and cytoplasm in columnar epithelial cells in epithelial adenocarcinoma, and the nucleus of invasive adenocarcinoma. (D) In the endometrial epithelium, YAP localises to the cytoplasm of columnar epithelial cells in epithelial adenocarcinoma, and the nucleus of invasive adenocarcinoma cells. (E) In urothelial epithelium, YAP localises to the cytoplasm in pseudostratified columnar cells in epithelial adenocarcinoma and to the nucleus of invasive adenocarcinoma. (F) YAP localises to the cytoplasm in ovarian adenocarcinoma, and to the nucleus of invasive ovarian adenocarcinoma. (G) YAP staining in $Apc^{-/-}$ $p53^{-/-}$ tumour organoids implanted subcutaneously into nude mice, which invade dramatically into the surrounding tissue. Note that cells at the invasive front feature nuclear YAP localisation, whereas columnar epithelial cells in the central regions of the tumour feature cytoplasmic YAP localisation. (H) YAP staining is strongly reduced by Dasatinib treatment of $Apc^{-/-}$ $p53^{-/-}$ tumour organoids implanted subcutaneously into nude mice. Invasive tumour cells are not visible. Quantification of YAP nuclear localisation was performed on n=200 tumour cells from G and H. Values are means±s.e.m.

no visible phenotype, confirming that the two proteins act in a redundant fashion in this tissue.

Both YAP and TAZ localise to the nucleus in the basal layer cells of the skin and we focused on YAP to characterize the molecular mechanisms responsible for this nuclear localisation (Figs 3–5). We examined the model that integrin-Src and EGFR-PI3K signalling promotes YAP nuclear localisation, which was first proposed based on experiments in MCF10A breast cells in culture (Fan et al., 2013; Kim and Gumbiner, 2015), and found that these signalling molecules are indeed strongly expressed in basal layer skin cells and are essential to promote YAP nuclear localisation in keratinocytes in culture and in mouse basal layer skin cells *in vivo*. Since YAP appears to induce expression of integrins, integrin ligands (CYR61, CTGF) and EGFR ligands (AREG), we propose that a positive feedback loop drives basal layer stem/progenitor cell identity and that this loop is broken when daughter cells lose contact with the basement membrane and differentiate – forming a bistable system of cell fate determination. Our findings provide an explanation for how these signalling pathways integrate to control skin stem/progenitor cell biology.

The notion that nuclear localisation of YAP occurs upon contact with basement membrane extracellular matrix applies equally to other squamous epithelia. By contrast, columnar epithelia differentiate an apical domain that induces YAP relocalisation to the cytoplasm via apical CRB3-MER-KIBRA-SAV signals, which are known to activate the MST and LATS kinases to promote YAP phosphorylation and cytoplasmic retention despite contact with the basement membrane (Figs 6, 7, Figs S4-S6) (Baumgartner et al., 2010; Chen et al., 2010; Fletcher et al., 2015; Genevet et al., 2010; Hamaratoglu et al., 2006; Ling et al., 2010; Sun et al., 2015; Szymaniak et al., 2015; Varelas et al., 2010; Yin et al., 2013; Yu et al., 2010). The CRB3-MER-KIBRA-SAV complex appears to be

Development (2016) 143, 1674-1687 doi:10.1242/dev.133728

absent in squamous epithelia, which never differentiate a true apical domain, leaving basement membrane contact as the sole regulatory mechanism (Fig. 6). Thus, our results show that antagonistic apical and basal polarity signals serve as the primary control mechanism that determines YAP subcellular localisation *in vivo*. In a striking parallel, the same apical and basal polarity determinants act antagonistically in epithelial membrane polarisation, with integrin and PI3K signalling localising PtdIns(3,4,5)P3 basally, and helping to restrict and/or orient PtdIns(4,5)P2, CDC42 and the CRB3 complex apically (Akhtar and Streuli, 2013; Bryant et al., 2014; Fletcher et al., 2012; Martin-Belmonte et al., 2007; Thompson, 2013). Further work will be necessary to fully elaborate the molecular interactions that mediate the antagonistic relationship between apical and basal signals in cell polarisation and nuclear signalling via YAP.

This fundamental control mechanism appears to be conserved across the animal kingdom. For example, *Drosophila* simple columnar epithelia such as imaginal discs rely primarily on apical Crb-Mer/Ex-Kibra-Sav signalling to retain Yki in the cytoplasm and restrict tissue growth (Baumgartner et al., 2010; Chen et al., 2010; Genevet et al., 2010; Hamaratoglu et al., 2006; Ling et al., 2010; Yu et al., 2010). By contrast, *Drosophila* stratified columnar epithelia such as the intestine require integrins, Src, EGFR and Yki to promote proliferation of basal layer stem/progenitor cells, suggesting that the regulatory connection between them described here is also conserved (Cordero et al., 2014; Jiang et al., 2011; Kohlmaier et al., 2015; Lin et al., 2013; Shaw et al., 2010; Staley and Irvine, 2010; Xu et al., 2011). Furthermore, ectopic activation of Src, EGFR, PI3K or Yki in simple columnar imaginal discs is sufficient to induce overproliferation of cells, whereas loss of PI3K or Yki strongly impairs imaginal disc tumour formation (Doggett et al., 2011; Enomoto and Igaki, 2013; Fernandez et al., 2014; Herranz et al., 2012, 2014; Strassburger et al., 2012; Willecke et al., 2011).

Our model raises interesting questions about the possible physiological roles of other YAP regulators identified in cell culture, namely that YAP is controlled by Wnt signalling (Azzolin et al., 2014; Cai et al., 2015; Park et al., 2015), GPCR signalling (Yu et al., 2012), PKA signalling (Yu et al., 2013), LKB1-MARK signalling (Mohseni et al., 2014), protease-activated receptors (Mo et al., 2012) or the Mevalonate pathway (Sorrentino et al., 2014). Further work is necessary to understand in which tissues and under what conditions these diverse signals are utilised and integrated *in vivo*.

Importantly, our model is easily reconciled with a possible role of YAP as a mechanosensor in epithelial tissues *in vivo* (Dupont et al., 2011). Mechanical force has been proposed to modulate signalling by both the apical Crb-Mer/Ex-Kibra-Sav system in *Drosophila* (Fletcher et al., 2015; Rauskolb et al., 2014) as well as the basal integrin-Src system in mammalian cell culture (reviewed in Humphrey et al., 2014; Lawson and Burridge, 2014). In the early mouse pre-implantation embryo, cortical tension is higher in outer cells than inner cells, leading to nuclear YAP in outer cells despite the presence of an apical domain (Anani et al., 2014; Kono et al., 2014; Nishioka et al., 2009). Consistently, reducing cortical tension with a ROCK inhibitor abolishes nuclear localisation of YAP in early mouse embryos (Anani et al., 2014; Kono et al., 2014; Nishioka et al., 2009). Mechanical forces might also explain why YAP becomes nuclear in some terminally differentiating and extremely flattened keratinocytes (Fig. 5, cells marked by asterisk).

Finally, our model is also easily reconciled with the ability of YAP to respond to inflammatory cues in epithelia, such as interleukin-6 (IL-6). Recent work revealed that the IL-6 co-receptor gp130 triggers stabilisation and nuclear translocation of YAP via Src kinases (Taniguchi et al., 2015). This signalling module was shown to be activated by mucosal injury to intestinal epithelia to promote intestinal regeneration, a known Src and YAP function (Cai et al., 2010; Cordero et al., 2014; Taniguchi et al., 2015). We confirm that tissue damage (with 14Gy of radiation) elevates YAP levels in a Src-dependent manner in the intestine (Fig. S7). However, we note that upon damage, localisation of YAP is still mostly nuclear in basal crypt stem cells, which normally lack an apical domain, and mostly cytoplasmic in differentiated columnar epithelial cells, which have an apical domain (Fig. S7). Interestingly, hyperproliferation per se driven by conditional deletion of APC and oncogenic mutation of KRAS (*VillinCreER* $Apc^{fl/fl}$ $K\text{-}ras^{LSL\text{-}G12D}$) does not change the fundamental pattern of YAP localisation, with localisation of YAP remaining most strongly nuclear in the basal stem cells but not the columnar epithelial cells (Fig. S6). In the skin, YAP is also elevated upon wounding (Fig. 2C,D) or inflammation (upon TPA treatment) in a Src-dependent manner (Fig. 5), but remains most strongly nuclear in the basal layer stem/progenitor cell population (Fig. 5). Thus, Src acts as a point of convergence between inflammatory cues and apical-basal polarity cues, with polarity cues being the dominant input. Further work is necessary to understand whether Src acts primarily by directly phosphorylating YAP or indirectly via enhancing PI3K signalling to inhibit MST-LATS activity. Nevertheless, our findings add weight to the notion that chemical inhibitors of Src kinases such as Dasatinib are promising cancer therapeutics (Creedon and Brunton, 2012; Karim et al., 2013) (Fig. 8).

In conclusion, epithelial stem/progenitor cell proliferation and differentiation might be regulated primarily by apical-basal polarity signals. In particular, YAP, a key driver of cell proliferation in stem/progenitor cells and cancer, appears to act primarily as a sensor of epithelial cell polarity and only secondarily as a sensor of other stimuli. Stem/progenitor cells thus use information about their polarity status to inform their decisions to either proliferate or arrest/differentiate via control of YAP. In the skin epithelium, nuclear YAP acts redundantly with TAZ to drive gene expression in the basal stem/progenitor cell layer to maintain cell proliferation and normal tissue homeostasis.

MATERIALS AND METHODS

Mouse strains

All experiments were carried out in accordance with the United Kingdom Animal Scientific Procedures Act (1986) and UK Home Office regulations under project licence number 70/7926. The $Yap^{fl/fl}$ $Taz^{fl/fl}$ mice were a gift from Axel Behrens (Francis Crick Institute). *K5-CreERt* mice were obtained from Ian Rosewell (Francis Crick Institute). *v-HA-Ras* transgene (TG.AC) mice were a gift from Ilaria Malanchi (Francis Crick Institute) and have been previously described (Leder et al., 1990). Wild-type mice were used in mixed background. All transgenic mice were in mixed background and used with littermate controls. APC p53 tumour sections from implanted nude mice were obtained from Owen Sansom (The Beatson Institute). *K14-Cre* $Fak^{fl/fl}$ mice and $Src^{fl/fl}$, $Fyn^{-/-}$, $Yes^{-/-}$ mice were obtained from Val Brunton (University of Edinburgh) and were described previously (Marcotte et al., 2012; Ridgway et al., 2012). $Apc^{-/-}$ $p53^{-/-}$ ($Apc^{580D/580D}$ *P53* $Trp53\Delta^{2-10}$ allele) mice were obtained from Owen Sansom and were previously described (Jonkers et al., 2001; Shibata et al., 1997). *AhCre* is previously described (Ireland et al., 2004). $K\text{-}ras^{G12D}$ allele is from Tyler Jacks (Jackson et al., 2001).

siRNA treatment

Human Caco-2, A431 or HaCAT cells were cultured as previously stated (Fletcher et al., 2015; Elbediwy et al., 2012). All siRNA transfections

Development (2016) 143, 1674-1687 doi:10.1242/dev.133728

were performed using Lipofectamine RNAiMax transfection reagent (Invitrogen). Briefly, cells were seeded in 6-well plates and treated with the siRNA/transfection mix 2 h post seeding. A final concentration of 50-100 nM siRNA was used for transfections. The following day, another transfection was performed before the cells were trypsinised 4 h later and reseeded either for 2D or 3D culture. 2D siRNA treatments were left for a total of 72 h and 3D treatments were left for a total of 120 h. 3D cultures were prepared as previously stated (Elbediwy et al., 2012). siRNAs were used as siGenome pools (Dharmacon).

Treatment with inhibitor, blocking antibody and low-calcium medium

2D mammalian inhibitor treatments were for 4 h. They were as follows: 5 µM PF573228 (FAK); 5 µM Saracatinib (Src); 5 µM Dasatinib (Src/Abl); 5 µM BX795 (PDK1); 5 µM MK2206 (AKT); 2 µM GDC0941 (PI3K); 100 µM Blebbistatin (myosin); 100 µM Y27632 (Rock); 2 µM Latrunculin A (actin) and 3 µM Everolimus (mTOR); reagents were supplied by Sigma-Aldrich and Stratech Scientific Ltd. Integrin β1 blocking antibody or control IgG antibody (gifts from Nancy Hogg, Francis Crick Institute) was incubated with the cells for 1 h at a concentration of 10 µg/ml before the cells were replated. Low-calcium conditions were as previously reported (Elbediwy et al., 2012). 2D wound healing involved plating the cells at high density, causing a scratch and subsequent addition of Dasatinib for 4 h.

Antibodies, image acquisition and quantification

Primary antibodies used were: rabbit YAP (H-125, Santa Cruz, sc-15407; 1:200IF, 1:1000 IB), mouse YAP (63.7; Santa Cruz, sc-101199; 1:200 IF, 1:1000 IB), rabbit p-YAP (Cell Signaling Technology, 4911; 1:1000 IB). Samples were imaged with a Leica SP5 confocal microscope using a 63× oil immersion objective and processed using Adobe Photoshop. Fixation and cell culture quantification was carried out as previously described (Fletcher et al., 2015).

YAP/TAZ conditional deletion

Tamoxifen (Sigma, 20 mg/ml in peanut oil) was injected intraperitoneally (IP) (5 µl/g body weight) for 5 consecutive days into 8- to 16-week-old controls or transgenic animals carrying *K5-CreERt Yap$^{fl/fl}$ Taz$^{fl/fl}$* to induce Yap/Taz knockdown and analysed for Yap/Taz deficiency by immunohistochemistry 7 days thereafter. *K5-CreERt Yap$^{fl/fl}$ Taz$^{fl/fl}$* mice used for long-term analysis were subsequently IP injected with tamoxifen every month for 3 consecutive days and analysed 8 weeks after the start of tamoxifen treatment.

Wound healing

Following the 5-day tamoxifen treatment, 4 hydroxy-tamoxifen (4OHT, Sigma) was topically applied to shaved back skin for 5 consecutive days at a dosage of 10 mg/ml in ethanol and 100 µl was applied per mouse. Mice were anaesthetised with IsoFlo (Isoflurane, Abbott Animal Health) and treated with the analgesics Vetergesic (Alstoe Animal Health) and Rimadyl (Pfizer Animal Health) for 2 days after wounding. A 4 mm punch wound was made in the back skin using a biopsy punch (Miltex) 10 days after tamoxifen/4OHT treatment start and wound closure monitored over time.

Dasatinib treatment of skin

Wild-type mice between 8 and 12 weeks of age were topically treated with 150 µl Dasatinib (10 µM in DMSO, Selleck) onto the shaved back skin directly followed by 200 µl TPA (12-O-tetradecanoylphorbol-13-acetate; stock dissolved in DMSO and diluted in acetone, 12.5 µg/mouse) treatment for 2 consecutive days. Mice were analysed and the back skin harvested on the third day. Control mice were treated with DMSO and acetone.

Chemical carcinogenesis

Chemical skin carcinogenesis was induced on 12-week-old *v-Ha-Ras* transgene (TG.AC)-expressing mice in mixed background by a single application of 100 µg/mouse DMBA [7,12-dimethylbenz(a)anthracene, Sigma] onto the shaved backskin followed by biweekly topical treatments with TPA (4 µg/mouse) starting 1 week after DMBA application. Skin papillomas were detectable 8 weeks after start of DMBA-TPA treatment and harvested at 13 weeks. For Dasatinib treatment, papillomas allowed to reach ∼1 cm^3. These established papillomas were treated topically with Dasatinib (10 µM in DMSO/acetone; 100 µl/papilloma) once and analysed 3 or 7 days thereafter. For generation of skin carcinomas, ∼12-week-old DMBA-treated FVB/N wild-type mice were treated biweekly with 4 µg/mouse TPA onto shaved back skin for 10 weeks then weekly for a further 4 weeks before the carcinomas were harvested.

Intestinal experiments

Mice carrying the *AhCre* recombinase were induced by three intraperitoneal (i.p.) injections of 80 mg/kg β-Napthoflavone for 1 day. Intestinal phenotypes were analysed 4 or 7 days after transgene induction to assess homeostasis or regeneration, respectively. Intestinal regeneration was induced by irradiating mice with 14Gy gamma-irradiation 4 days after recombinase induction. Mice were sacrificed 72 h post irradiation and the small intestine isolated and flushed with tap water. Ten 1 cm portions of small intestine were bound together with surgical tape and fixed in 4% neutral buffered formalin.

Organoid transplantation experiments

Intestinal crypts from *VillinCreER Apc$^{fl/fl}$ p53$^{fl/fl}$* mice were removed 4 days following Cre induction with Tamoxifen (2 mg). This causes full recombination at both the *Apc* and *p53* loci and organoids now grow as spheres in an R-Spondin-independent manner (Sato et al., 2009). For transplantation of organoids, 50 organoids were transplanted subcutaneously into nude mice (see Valeri et al., 2014). A dose of 10 mg/kg Dasatinib daily gavage was chosen as we have previously shown to cause a reduction in p-SRC *in vivo* without toxicity (Morton et al., 2010). Mice were treated continuously from 10 days post injection of spheres.

Immunohistochemistry

Mouse back skin samples were harvested and fixed in neutral-buffered formaldehyde 10% v/v and then embedded in paraffin blocks. 4-µm-thick sections were cut, deparaffinised and rehydrated using standard methods. After an antigen retrieval step, sections were stained with Hematoxylin and Eosin (H&E) solution or with primary antibody. Additional images of human samples were obtained by datamining the www.proteinatlas.org database (Berglund et al., 2008; Lundberg and Uhlén, 2010; Pontén et al., 2008; Uhlen et al., 2005, 2015, 2010).

RNA-seq analysis

A431 or HaCAT cell lysates transfected with empty vector, YAP1 S5A, control siRNA or YAP1 siRNAs were used. Sequencing was performed on biological triplicates on the Illumina HiSeq 2500 platform and generated ∼69 million 100 bp paired end reads per sample (data deposited in GEO under accession number GSE80082). Sequenced reads were trimmed to 75 base pairs and mapped to the Refseq genome model, using RSEM (v.1.2.21). RSEM uses the bowtie2 alignment tool. Gene counts were filtered to remove genes with 10 or fewer mapped reads per sample. TMM (treated mean of M-values) normalisation and differential expression analysis using the negative binomial model was carried out with the R-Bioconductor package 'EdgeR'. Genes with logCPM>1 and FDR<0.05 were judged to be differentially expressed. Enrichments of pathway, category and motif gene sets were assessed using GSEA with logFC pre-ranked gene lists. Gene sets with an enrichment false discovery rate (FDR) value of less than 0.05 were judged to be strongly statistically significant and values of less than 0.25 significant.

qPCR

Total RNA was extracted from homogenised mouse skin using an RNeasy Mini Kit (Qiagen). cDNA synthesis for WT or dKO mice was performed using Superscript II (Invitrogen). Primers were purchased as Quantitect Primers (Qiagen). Gene samples were run in triplicate on a Quantstudio 12 Flex Thermocycler. Expression values were calculated using the ΔΔCT method relative to the housekeeping gene β-2-microglobulin (B2M). All error bars indicate s.e.m.

Development (2016) 143, 1674-1687 doi:10.1242/dev.133728

Acknowledgements
We thank Jimmy Hu and Ophir Klein for discussions of the K14-Cre YAP/TAZ dKO phenotype. We thank Elanor Wainwright for providing mouse skin papillomas. We thank Nancy Hogg for providing Integrin β1 blocking antibody and Nic Tapon for comments on the manuscript.

Competing interests
The authors declare no competing or financial interests.

Author contributions
A.E., Z.I.V.-M. and B.J.T. designed research, planned experiments and analysed the data; A.E. performed mammalian cell cuture experiments and RT-PCR; Z.V.M performed the mouse experiments. A.E. and Z.I.V.-M. performed the RNA-seq. S.B. analysed the RNA-seq and prepared the data. B.S.-D and R.K.S stained and prepared the tissue sections; J.C., E.H.T., R.R., V.G.B., E.S., H.G., A.B., I.M. and O.J.S. provided tissue samples and reagents; S.K.W. assisted with some mouse experiments. B.J.T. along with input from the other authors wrote the manuscript.

Funding
This research was funded by the Francis Crick Institute, Cancer Research UK and the Wellcome Trust. Deposited in PMC for immediate release.

Data availability
RNA-seq data has been deposited in Gene Expression Omnibus (GEO) under accession number GSE80082 and is available at http://www.ncbi.nlm.nih.gov/geo/query/acc.cgi?acc=GSE80082.

Supplementary information
Supplementary information available online at
http://dev.biologists.org/lookup/suppl/doi:10.1242/dev.133728/-/DC1

References

Akhtar, N. and Streuli, C. H. (2013). An integrin–ILK–microtubule network orients cell polarity and lumen formation in glandular epithelium. *Nat. Cell Biol.* **15**, 17-27.
Anani, S., Bhat, S., Honma-Yamanaka, N., Krawchuk, D. and Yamanaka, Y. (2014). Initiation of Hippo signaling is linked to polarity rather than to cell position in the pre-implantation mouse embryo. *Development* **141**, 2813-2824.
Aragona, M., Panciera, T., Manfrin, A., Giulitti, S., Michielin, F., Elvassore, N., Dupont, S. and Piccolo, S. (2013). A mechanical checkpoint controls multicellular growth through YAP/TAZ regulation by actin-processing factors. *Cell* **154**, 1047-1059.
Azzolin, L., Panciera, T., Soligo, S., Enzo, E., Bicciato, S., Dupont, S., Bresolin, S., Frasson, C., Basso, G., Guzzardo, V. et al. (2014). YAP/TAZ incorporation in the beta-catenin destruction complex orchestrates the Wnt response. *Cell* **158**, 157-170.
Baumgartner, R., Poernbacher, I., Buser, N., Hafen, E. and Stocker, H. (2010). The WW domain protein Kibra acts upstream of Hippo in Drosophila. *Dev. Cell* **18**, 309-316.
Benham-Pyle, B. W., Pruitt, B. L. and Nelson, W. J. (2015). Cell adhesion. Mechanical strain induces E-cadherin-dependent Yap1 and beta-catenin activation to drive cell cycle entry. *Science* **348**, 1024-1027.
Berglund, L., Bjorling, E., Oksvold, P., Fagerberg, L., Asplund, A., Szigyarto, C. A.-K., Persson, A., Ottosson, J., Wernerus, H., Nilsson, P. et al. (2008). A genecentric Human Protein Atlas for expression profiles based on antibodies. *Mol. Cell. Proteomics* **7**, 2019-2027.
Brakebusch, C., Grose, R., Quondamatteo, F., Ramirez, A., Jorcano, J. L., Pirro, A., Svensson, M., Herken, R., Sasaki, T., Timpl, R. et al. (2000). Skin and hair follicle integrity is crucially dependent on beta 1 integrin expression on keratinocytes. *EMBO J.* **19**, 3990-4003.
Bryant, D. M., Roignot, J., Datta, A., Overeem, A. W., Kim, M., Yu, W., Peng, X., Eastburn, D. J., Ewald, A. J., Werb, Z. et al. (2014). A molecular switch for the orientation of epithelial cell polarization. *Dev. Cell* **31**, 171-187.
Cai, J., Zhang, N., Zheng, Y., de Wilde, R. F., Maitra, A. and Pan, D. (2010). The Hippo signaling pathway restricts the oncogenic potential of an intestinal regeneration program. *Genes Dev.* **24**, 2383-2388.
Cai, J., Maitra, A., Anders, R. A., Taketo, M. M. and Pan, D. (2015). beta-Catenin destruction complex-independent regulation of Hippo–YAP signaling by APC in intestinal tumorigenesis. *Genes Dev.* **29**, 1493-1506.
Camargo, F. D., Gokhale, S., Johnnidis, J. B., Fu, D., Bell, G. W., Jaenisch, R. and Brummelkamp, T. R. (2007). YAP1 increases organ size and expands undifferentiated progenitor cells. *Curr. Biol.* **17**, 2054-2060.
Chen, C.-L., Gajewski, K. M., Hamaratoglu, F., Bossuyt, W., Sansores-Garcia, L., Tao, C. and Halder, G. (2010). The apical-basal cell polarity determinant Crumbs regulates Hippo signaling in Drosophila. *Proc. Natl. Acad. Sci. USA* **107**, 15810-15815.
Cho, E., Feng, Y., Rauskolb, C., Maitra, S., Fehon, R. and Irvine, K. D. (2006). Delineation of a Fat tumor suppressor pathway. *Nat. Genet.* **38**, 1142-1150.
Cordero, J. B., Ridgway, R. A., Valeri, N., Nixon, C., Frame, M. C., Muller, W. J., Vidal, M. and Sansom, O. J. (2014). c-Src drives intestinal regeneration and transformation. *EMBO J.* **33**, 1474-1491.
Creedon, H. and Brunton, V. G. (2012). Src kinase inhibitors: promising cancer therapeutics? *Crit. Rev. Oncog.* **17**, 145-159.
Das Thakur, M., Feng, Y., Jagannathan, R., Seppa, M. J., Skeath, J. B. and Longmore, G. D. (2010). Ajuba LIM proteins are negative regulators of the Hippo signaling pathway. *Curr. Biol.* **20**, 657-662.
Degoutin, J. L., Milton, C. C., Yu, E., Tipping, M., Bosveld, F., Yang, L., Bellaiche, Y., Veraksa, A. and Harvey, K. F. (2013). Riquiqui and minibrain are regulators of the Hippo pathway downstream of Dachsous. *Nat. Cell Biol.* **15**, 1176-1185.
Doggett, K., Grusche, F. A., Richardson, H. E. and Brumby, A. M. (2011). Loss of the Drosophila cell polarity regulator Scribbled promotes epithelial tissue overgrowth and cooperation with oncogenic Ras-Raf through impaired Hippo pathway signaling. *BMC Dev. Biol.* **11**, 57.
Dong, J., Feldmann, G., Huang, J., Wu, S., Zhang, N., Comerford, S. A., Gayyed, M. F., Anders, R. A., Maitra, A. and Pan, D. (2007). Elucidation of a universal size-control mechanism in Drosophila and mammals. *Cell* **130**, 1120-1133.
Dupont, S., Morsut, L., Aragona, M., Enzo, E., Giulitti, S., Cordenonsi, M., Zanconato, F., Le Digabel, J., Forcato, M., Bicciato, S. et al. (2011). Role of YAP/TAZ in mechanotransduction. *Nature* **474**, 179-183.
Elbediwy, A., Zihni, C., Terry, S. J., Clark, P., Matter, K. and Balda, M. S. (2012). Epithelial junction formation requires confinement of Cdc42 activity by a novel SH3BP1 complex. *J. Cell Biol.* **198**, 677-693.
Enomoto, M. and Igaki, T. (2013). Src controls tumorigenesis via JNK-dependent regulation of the Hippo pathway in Drosophila. *EMBO Rep.* **14**, 65-72.
Fan, R., Kim, N.-G. and Gumbiner, B. M. (2013). Regulation of Hippo pathway by mitogenic growth factors via phosphoinositide 3-kinase and phosphoinositide-dependent kinase-1. *Proc. Natl. Acad. Sci. USA* **110**, 2569-2574.
Fernandez, B. G., Gaspar, P., Bras-Pereira, C., Jezowska, B., Rebelo, S. R. and Janody, F. (2011). Actin-Capping Protein and the Hippo pathway regulate F-actin and tissue growth in Drosophila. *Development* **138**, 2337-2346.
Fernandez, B. G., Jezowska, B. and Janody, F. (2014). Drosophila actin-Capping Protein limits JNK activation by the Src proto-oncogene. *Oncogene* **33**, 2027-2039.
Fletcher, G. C., Lucas, E. P., Brain, R., Tournier, A. and Thompson, B. J. (2012). Positive feedback and mutual antagonism combine to polarize Crumbs in the Drosophila follicle cell epithelium. *Curr. Biol.* **22**, 1116-1122.
Fletcher, G. C., Elbediwy, A., Khanal, I., Ribeiro, P. S., Tapon, N. and Thompson, B. J. (2015). The Spectrin cytoskeleton regulates the Hippo signalling pathway. *EMBO J.* **34**, 940-954.
Gaspar, P., Holder, M. V., Aerne, B. L., Janody, F. and Tapon, N. (2015). Zyxin antagonizes the FERM protein expanded to couple F-actin and Yorkie-dependent organ growth. *Curr. Biol.* **25**, 679-689.
Genevet, A., Wehr, M. C., Brain, R., Thompson, B. J. and Tapon, N. (2010). Kibra is a regulator of the Salvador/Warts/Hippo signaling network. *Dev. Cell* **18**, 300-308.
Grose, R., Hutter, C., Bloch, W., Thorey, I., Watt, F. M., Fassler, R., Brakebusch, C. and Werner, S. (2002). A crucial role of beta 1 integrins for keratinocyte migration in vitro and during cutaneous wound repair. *Development* **129**, 2303-2315.
Hamaratoglu, F., Willecke, M., Kango-Singh, M., Nolo, R., Hyun, E., Tao, C., Jafar-Nejad, H. and Halder, G. (2006). The tumour-suppressor genes NF2/Merlin and Expanded act through Hippo signalling to regulate cell proliferation and apoptosis. *Nat. Cell Biol.* **8**, 27-36.
Harvey, K. F., Zhang, X. and Thomas, D. M. (2013). The Hippo pathway and human cancer. *Nat. Rev. Cancer* **13**, 246-257.
Herranz, H., Hong, X. and Cohen, S. M. (2012). Mutual repression by bantam miRNA and Capicua links the EGFR/MAPK and Hippo pathways in growth control. *Curr. Biol.* **22**, 651-657.
Herranz, H., Weng, R. and Cohen, S. M. (2014). Crosstalk between epithelial and mesenchymal tissues in tumorigenesis and imaginal disc development. *Curr. Biol.* **24**, 1476-1484.
Huang, J., Wu, S., Barrera, J., Matthews, K. and Pan, D. (2005). The Hippo signaling pathway coordinately regulates cell proliferation and apoptosis by inactivating Yorkie, the Drosophila Homolog of YAP. *Cell* **122**, 421-434.
Humphrey, J. D., Dufresne, E. R. and Schwartz, M. A. (2014). Mechanotransduction and extracellular matrix homeostasis. *Nat. Rev. Mol. Cell Biol.* **15**, 802-812.
Ireland, H., Kemp, R., Houghton, C., Howard, L., Clarke, A. R., Sansom, O. J. and Winton, D. J. (2004). Inducible Cre-mediated control of gene expression in the murine gastrointestinal tract: effect of loss of beta-catenin. *Gastroenterology* **126**, 1236-1246.
Irvine, K. D. and Harvey, K. F. (2015). Control of organ growth by patterning and Hippo signaling in Drosophila. *Cold Spring Harb. Perspect. Biol.* **7**, a019224.
Jackson, E. L., Willis, N., Mercer, K., Bronson, R. T., Crowley, D., Montoya, R., Jacks, T. and Tuveson, D. A. (2001). Analysis of lung tumor initiation and progression using conditional expression of oncogenic K-ras. *Genes Dev.* **15**, 3243-3248.

Jiang, H., Grenley, M. O., Bravo, M.-J., Blumhagen, R. Z. and Edgar, B. A. (2011). EGFR/Ras/MAPK signaling mediates adult midgut epithelial homeostasis and regeneration in Drosophila. *Cell Stem Cell* **8**, 84-95.
Jin, Y., Xu, J., Yin, M.-X., Lu, Y., Hu, L., Li, P., Zhang, P., Yuan, Z., Ho, M. S., Ji, H. et al. (2013). Brahma is essential for Drosophila intestinal stem cell proliferation and regulated by Hippo signaling. *eLife* **2**, e00999.
Jonkers, J., Meuwissen, R., van der Gulden, H., Peterse, H., van der Valk, M. and Berns, A. (2001). Synergistic tumor suppressor activity of BRCA2 and p53 in a conditional mouse model for breast cancer. *Nat. Genet.* **29**, 418-425.
Karim, S. A., Creedon, H., Patel, H., Carragher, N. O., Morton, J. P., Muller, W. J., Evans, T. R., Gusterson, B., Sansom, O. J. and Brunton, V. G. (2013). Dasatinib inhibits mammary tumour development in a genetically engineered mouse model. *J. Pathol.* **230**, 430-440.
Kim, N.-G. and Gumbiner, B. M. (2015). Adhesion to fibronectin regulates Hippo signaling via the FAK–Src–PI3K pathway. *J. Cell Biol.* **210**, 503-515.
Kohlmaier, A., Fassnacht, C., Jin, Y., Reuter, H., Begum, J., Dutta, D. and Edgar, B. A. (2015). Src kinase function controls progenitor cell pools during regeneration and tumor onset in the Drosophila intestine. *Oncogene* **34**, 2371-2384.
Kono, K., Tamashiro, D. A. and Alarcon, V. B. (2014). Inhibition of RHO–ROCK signaling enhances ICM and suppresses TE characteristics through activation of Hippo signaling in the mouse blastocyst. *Dev. Biol.* **394**, 142-155.
Koontz, L. M., Liu-Chittenden, Y., Yin, F., Zheng, Y., Yu, J., Huang, B., Chen, Q., Wu, S. and Pan, D. (2013). The Hippo effector Yorkie controls normal tissue growth by antagonizing scalloped-mediated default repression. *Dev. Cell* **25**, 388-401.
Lawson, C. D. and Burridge, K. (2014). The on-off relationship of Rho and Rac during integrin-mediated adhesion and cell migration. *Small GTPases* **5**, e27958.
Leder, A., Kuo, A., Cardiff, R. D., Sinn, E. and Leder, P. (1990). v-Ha-ras transgene abrogates the initiation step in mouse skin tumorigenesis: effects of phorbol esters and retinoic acid. *Proc. Natl. Acad. Sci. USA* **87**, 9178-9182.
Lin, G., Zhang, X., Ren, J., Pang, Z., Wang, C., Xu, N. and Xi, R. (2013). Integrin signaling is required for maintenance and proliferation of intestinal stem cells in Drosophila. *Dev. Biol.* **377**, 177-187.
Ling, C., Zheng, Y., Yin, F., Yu, J., Huang, J., Hong, Y., Wu, S. and Pan, D. (2010). The apical transmembrane protein Crumbs functions as a tumor suppressor that regulates Hippo signaling by binding to Expanded. *Proc. Natl. Acad. Sci. USA* **107**, 10532-10537.
Liu-Chittenden, Y., Huang, B., Shim, J. S., Chen, Q., Lee, S.-J., Anders, R. A., Liu, J. O. and Pan, D. (2012). Genetic and pharmacological disruption of the TEAD-YAP complex suppresses the oncogenic activity of YAP. *Genes Dev.* **26**, 1300-1305.
Lundberg, E. and Uhlén, M. (2010). Creation of an antibody-based subcellular protein atlas. *Proteomics* **10**, 3984-3996.
Mao, Y., Rauskolb, C., Cho, E., Hu, W.-L., Hayter, H., Minihan, G., Katz, F. N. and Irvine, K. D. (2006). Dachs: an unconventional myosin that functions downstream of Fat to regulate growth, affinity and gene expression in Drosophila. *Development* **133**, 2539-2551.
Marcotte, R., Smith, H. W., Sanguin-Gendreau, V., McDonough, R. V. and Muller, W. J. (2012). Mammary epithelial-specific disruption of c-Src impairs cell cycle progression and tumorigenesis. *Proc. Natl. Acad. Sci. USA* **109**, 2808-2813.
Martin-Belmonte, F., Gassama, A., Datta, A., Yu, W., Rescher, U., Gerke, V. and Mostov, K. (2007). PTEN-mediated apical segregation of phosphoinositides controls epithelial morphogenesis through Cdc42. *Cell* **128**, 383-397.
Mo, J.-S., Yu, F.-X., Gong, R., Brown, J. H. and Guan, K.-L. (2012). Regulation of the Hippo-YAP pathway by protease-activated receptors (PARs). *Genes Dev.* **26**, 2138-2143.
Mohseni, M., Sun, J., Lau, A., Curtis, S., Goldsmith, J., Fox, V. L., Wei, C., Frazier, M., Samson, O., Wong, K.-K. et al. (2014). A genetic screen identifies an LKB1–MARK signalling axis controlling the Hippo–YAP pathway. *Nat. Cell Biol.* **16**, 108-117.
Morton, J. P., Karim, S. A., Graham, K., Timpson, P., Jamieson, N., Athineos, D., Doyle, B., McKay, C., Heung, M.-Y., Oien, K. A. et al. (2010). Dasatinib inhibits the development of metastases in a mouse model of pancreatic ductal adenocarcinoma. *Gastroenterology* **139**, 292-303.
Nishioka, N., Inoue, K.-i., Adachi, K., Kiyonari, H., Ota, M., Ralston, A., Yabuta, N., Hirahara, S., Stephenson, R. O., Ogonuki, N. et al. (2009). The Hippo signaling pathway components Lats and Yap pattern Tead4 activity to distinguish mouse trophectoderm from inner cell mass. *Dev. Cell* **16**, 398-410.
Oh, H. and Irvine, K. D. (2008). In vivo regulation of Yorkie phosphorylation and localization. *Development* **135**, 1081-1088.
Oh, H., Slattery, M., Ma, L., Crofts, A., White, K. P., Mann, R. S. and Irvine, K. D. (2013). Genome-wide association of Yorkie with chromatin and chromatin-remodeling complexes. *Cell Rep.* **3**, 309-318.
Pan, D. (2010). The Hippo signaling pathway in development and cancer. *Dev. Cell* **19**, 491-505.
Pan, D. (2015). YAPing Hippo forecasts a new target for lung cancer prevention and treatment. *J. Clin. Oncol.* **33**, 2311-2313.
Park, H. W., Kim, Y. C., Yu, B., Moroishi, T., Mo, J.-S., Plouffe, S. W., Meng, Z., Lin, K. C., Yu, F.-X., Alexander, C. M. et al. (2015). Alternative Wnt signaling activates YAP/TAZ. *Cell* **162**, 780-794.
Piccolo, S., Cordenonsi, M. and Dupont, S. (2013). Molecular pathways: YAP and TAZ take center stage in organ growth and tumorigenesis. *Clin. Cancer Res.* **19**, 4925-4930.
Piwko-Czuchra, A., Koegel, H., Meyer, H., Bauer, M., Werner, S., Brakebusch, C. and Fässler, R. (2009). Beta1 integrin-mediated adhesion signalling is essential for epidermal progenitor cell expansion. *PLoS ONE* **4**, e5488.
Pontén, F., Jirström, K. and Uhlen, M. (2008). The Human Protein Atlas-a tool for pathology. *J. Pathol.* **216**, 387-393.
Raghavan, S., Bauer, C., Mundschau, G., Li, Q. and Fuchs, E. (2000). Conditional ablation of beta1 integrin in skin. Severe defects in epidermal proliferation, basement membrane formation, and hair follicle invagination. *J. Cell Biol.* **150**, 1149-1160.
Rauskolb, C., Pan, G., Reddy, B. V. V. G., Oh, H. and Irvine, K. D. (2011). Zyxin links fat signaling to the Hippo pathway. *PLoS Biol.* **9**, e1000624.
Rauskolb, C., Sun, S., Sun, G., Pan, Y. and Irvine, K. D. (2014). Cytoskeletal tension inhibits Hippo signaling through an Ajuba-Warts complex. *Cell* **158**, 143-156.
Reginensi, A., Hoshi, M., Boualia, S. K., Bouchard, M., Jain, S. and McNeill, H. (2015). Yap and Taz are required for Ret-dependent urinary tract morphogenesis. *Development* **142**, 2696-2703.
Ridgway, R. A., Serrels, B., Mason, S., Kinnaird, A., Muir, M., Patel, H., Muller, W. J., Sansom, O. J. and Brunton, V. G. (2012). Focal adhesion kinase is required for beta-catenin-induced mobilization of epidermal stem cells. *Carcinogenesis* **33**, 2369-2376.
Sansores-Garcia, L., Bossuyt, W., Wada, K.-I., Yonemura, S., Tao, C., Sasaki, H. and Halder, G. (2011). Modulating F-actin organization induces organ growth by affecting the Hippo pathway. *EMBO J.* **30**, 2325-2335.
Sansores-Garcia, L., Atkins, M., Moya, I. M., Shahmoradgoli, M., Tao, C., Mills, G. B. and Halder, G. (2013). Mask is required for the activity of the Hippo pathway effector Yki/YAP. *Curr. Biol.* **23**, 229-235.
Sato, T., Vries, R. G., Snippert, H. J., van de Wetering, M., Barker, N., Stange, D. E., van Es, J. H., Abo, A., Kujala, P., Peters, P. J. et al. (2009). Single Lgr5 stem cells build crypt–villus structures in vitro without a mesenchymal niche. *Nature* **459**, 262-265.
Schlegelmilch, K., Mohseni, M., Kirak, O., Pruszak, J., Rodriguez, J. R., Zhou, D., Kreger, B. T., Vasioukhin, V., Avruch, J., Brummelkamp, T. R. et al. (2011). Yap1 acts downstream of alpha-catenin to control epidermal proliferation. *Cell* **144**, 782-795.
Serrels, B., Serrels, A., Mason, S. M., Baldeschi, C., Ashton, G. H., Canel, M., Mackintosh, L. J., Doyle, B., Green, T. P., Frame, M. C. et al. (2009). A novel Src kinase inhibitor reduces tumour formation in a skin carcinogenesis model. *Carcinogenesis* **30**, 249-257.
Shaw, R. L., Kohlmaier, A., Polesello, C., Veelken, C., Edgar, B. A. and Tapon, N. (2010). The Hippo pathway regulates intestinal stem cell proliferation during Drosophila adult midgut regeneration. *Development* **137**, 4147-4158.
Shibata, H., Toyama, K., Shioya, H., Ito, M., Hirota, M., Hasegawa, S., Matsumoto, H., Takano, H., Akiyama, T., Toyoshima, K. et al. (1997). Rapid colorectal adenoma formation initiated by conditional targeting of the Apc gene. *Science* **278**, 120-123.
Sidor, C. M., Brain, R. and Thompson, B. J. (2013). Mask proteins are cofactors of Yorkie/YAP in the Hippo pathway. *Curr. Biol.* **23**, 223-228.
Singh, P., Chen, C., Pal-Ghosh, S., Stepp, M. A., Sheppard, D. and Van De Water, L. (2009). Loss of integrin alpha9beta1 results in defects in proliferation, causing poor re-epithelialization during cutaneous wound healing. *J. Invest. Dermatol.* **129**, 217-228.
Sorrentino, G., Ruggeri, N., Specchia, V., Cordenonsi, M., Mano, M., Dupont, S., Manfrin, A., Ingallina, E., Sommaggio, R., Piazza, S. et al. (2014). Metabolic control of YAP and TAZ by the mevalonate pathway. *Nat. Cell Biol.* **16**, 357-366.
Staley, B. K. and Irvine, K. D. (2010). Warts and Yorkie mediate intestinal regeneration by influencing stem cell proliferation. *Curr. Biol.* **20**, 1580-1587.
Strassburger, K., Tiebe, M., Pinna, F., Breuhahn, K. and Teleman, A. A. (2012). Insulin/IGF signaling drives cell proliferation in part via Yorkie/YAP. *Dev. Biol.* **367**, 187-196.
Sun, S., Reddy, B. V. V. G. and Irvine, K. D. (2015). Localization of Hippo signalling complexes and Warts activation in vivo. *Nat. Commun.* **6**, 8402.
Szymaniak, A. D., Mahoney, J. E., Cardoso, W. V. and Varelas, X. (2015). Crumbs3-mediated polarity directs airway epithelial cell fate through the Hippo pathway effector yap. *Dev. Cell* **34**, 283-296.
Taniguchi, K., Wu, L.-W., Grivennikov, S. I., de Jong, P. R., Lian, I., Yu, F.-X., Wang, K., Ho, S. B., Boland, B. S., Chang, J. T. et al. (2015). A gp130–Src–YAP module links inflammation to epithelial regeneration. *Nature* **519**, 57-62.
Thompson, B. J. (2013). Cell polarity: models and mechanisms from yeast, worms and flies. *Development* **140**, 13-21.
Uhlen, M., Björling, E., Agaton, C., Szigyarto, C. A.-K., Amini, B., Andersen, E., Andersson, A.-C., Angelidou, P., Asplund, A., Asplund, C. et al. (2005). A

Development (2016) 143, 1674-1687 doi:10.1242/dev.133728

human protein atlas for normal and cancer tissues based on antibody proteomics. *Mol. Cell. Proteomics* **4**, 1920-1932.

Uhlen, M., Oksvold, P., Fagerberg, L., Lundberg, E., Jonasson, K., Forsberg, M., Zwahlen, M., Kampf, C., Wester, K., Hober, S. et al. (2010). Towards a knowledge-based Human Protein Atlas. *Nat. Biotechnol.* **28**, 1248-1250.

Uhlen, M., Fagerberg, L., Hallstrom, B. M., Lindskog, C., Oksvold, P., Mardinoglu, A., Sivertsson, A., Kampf, C., Sjostedt, E., Asplund, A. et al. (2015). Proteomics. Tissue-based map of the human proteome. *Science* **347**, 1260419.

Valeri, N., Braconi, C., Gasparini, P., Murgia, C., Lampis, A., Paulus-Hock, V., Hart, J. R., Ueno, L., Grivennikov, S. I., Lovat, F. et al. (2014). MicroRNA-135b promotes cancer progression by acting as a downstream effector of oncogenic pathways in colon cancer. *Cancer Cell* **25**, 469-483.

Varelas, X., Samavarchi-Tehrani, P., Narimatsu, M., Weiss, A., Cockburn, K., Larsen, B. G., Rossant, J. and Wrana, J. L. (2010). The Crumbs complex couples cell density sensing to Hippo-dependent control of the TGF-beta-SMAD pathway. *Dev. Cell* **19**, 831-844.

Vassilev, A., Kaneko, K. J., Shu, H., Zhao, Y. and DePamphilis, M. L. (2001). TEAD/TEF transcription factors utilize the activation domain of YAP65, a Src/Yes-associated protein localized in the cytoplasm. *Genes Dev.* **15**, 1229-1241.

Willecke, M., Toggweiler, J. and Basler, K. (2011). Loss of PI3K blocks cell-cycle progression in a Drosophila tumor model. *Oncogene* **30**, 4067-4074.

Wu, S., Liu, Y., Zheng, Y., Dong, J. and Pan, D. (2008). The TEAD/TEF family protein Scalloped mediates transcriptional output of the Hippo growth-regulatory pathway. *Dev. Cell* **14**, 388-398.

Xu, N., Wang, S. Q., Tan, D., Gao, Y., Lin, G. and Xi, R. (2011). EGFR, Wingless and JAK/STAT signaling cooperatively maintain Drosophila intestinal stem cells. *Dev. Biol.* **354**, 31-43.

Yin, F., Yu, J., Zheng, Y., Chen, Q., Zhang, N. and Pan, D. (2013). Spatial organization of Hippo signaling at the plasma membrane mediated by the tumor suppressor Merlin/NF2. *Cell* **154**, 1342-1355.

Yu, J., Zheng, Y., Dong, J., Klusza, S., Deng, W.-M. and Pan, D. (2010). Kibra functions as a tumor suppressor protein that regulates Hippo signaling in conjunction with Merlin and Expanded. *Dev. Cell* **18**, 288-299.

Yu, F.-X., Zhao, B., Panupinthu, N., Jewell, J. L., Lian, I., Wang, L. H., Zhao, J., Yuan, H., Tumaneng, K., Li, H. et al. (2012). Regulation of the Hippo-YAP pathway by G-protein-coupled receptor signaling. *Cell* **150**, 780-791.

Yu, F.-X., Zhang, Y., Park, H. W., Jewell, J. L., Chen, Q., Deng, Y., Pan, D., Taylor, S. S., Lai, Z.-C. and Guan, K.-L. (2013). Protein kinase A activates the Hippo pathway to modulate cell proliferation and differentiation. *Genes Dev.* **27**, 1223-1232.

Zanconato, F., Forcato, M., Battilana, G., Azzolin, L., Quaranta, E., Bodega, B., Rosato, A., Bicciato, S., Cordenonsi, M. and Piccolo, S. (2015). Genome-wide association between YAP/TAZ/TEAD and AP-1 at enhancers drives oncogenic growth. *Nat. Cell Biol.* **17**, 1218-1227.

Zhang, N., Bai, H., David, K. K., Dong, J., Zheng, Y., Cai, J., Giovannini, M., Liu, P., Anders, R. A. and Pan, D. (2010). The Merlin/NF2 tumor suppressor functions through the YAP oncoprotein to regulate tissue homeostasis in mammals. *Dev. Cell* **19**, 27-38.

Zhang, H., Pasolli, H. A. and Fuchs, E. (2011a). Yes-associated protein (YAP) transcriptional coactivator functions in balancing growth and differentiation in skin. *Proc. Natl. Acad. Sci. USA* **108**, 2270-2275.

Zhang, X., Milton, C. C., Poon, C. L. C., Hong, W. and Harvey, K. F. (2011b). Wbp2 cooperates with Yorkie to drive tissue growth downstream of the Salvador–Warts–Hippo pathway. *Cell Death Differ.* **18**, 1346-1355.

Zhao, B., Wei, X., Li, W., Udan, R. S., Yang, Q., Kim, J., Xie, J., Ikenoue, T., Yu, J., Li, L. et al. (2007). Inactivation of YAP oncoprotein by the Hippo pathway is involved in cell contact inhibition and tissue growth control. *Genes Dev.* **21**, 2747-2761.

Zhao, R., Fallon, T. R., Saladi, S. V., Pardo-Saganta, A., Villoria, J., Mou, H., Vinarsky, V., Gonzalez-Celeiro, M., Nunna, N., Hariri, L. P. et al. (2014). Yap tunes airway epithelial size and architecture by regulating the identity, maintenance, and self-renewal of stem cells. *Dev. Cell* **30**, 151-165.

NAME	link.to.category	FDR_logFC_SSA_YAP_A431.top.txt	FDR_logFC_siYAP_siCTRL_A431.bottom.txt	FDR_logFC_siYAP_siCTRL_HaCAT.bottom.txt
YAP signalling				
REACTOME_SIGNALING_BY_HIPPO	http://www.broadinstitute.org/gsea/msig	0.27403983	0.0845902	0.016429855
REACTOME_YAP1_AND_WWTR1_TAZ_STIMULATED_GENE_EXPRESSION	http://www.broadinstitute.org/gsea/msig	0.09720611	0.27879855	0.2792244
Cell cycle				
REACTOME_G1_S_TRANSITION	http://www.broadinstitute.org/gsea/msig	0.02010638	0	0.000541
REACTOME_MITOTIC_M_M_G1_PHASES	http://www.broadinstitute.org/gsea/msig	0.02990606	0.000957	0
REACTOME_DNA_REPLICATION	http://www.broadinstitute.org/gsea/msig	0.030264564	7.26E-05	0.004145181
ZHOU_CELL_CYCLE_GENES_IN_IR_RESPONSE_6HR	http://www.broadinstitute.org/gsea/msig	0.031962935	0	0.011136545
REACTOME_ORC1_REMOVAL_FROM_CHROMATIN	http://www.broadinstitute.org/gsea/msig	0.032863572	0.00102613	0.009737373
REACTOME_M_G1_TRANSITION	http://www.broadinstitute.org/gsea/msig	0.033798005	0	0
REACTOME_S_PHASE	http://www.broadinstitute.org/gsea/msig	0.034246594	0	0.005542807
REACTOME_SYNTHESIS_OF_DNA	http://www.broadinstitute.org/gsea/msig	0.04779358	0	0.005340172
REACTOME_CELL_CYCLE_CHECKPOINTS	http://www.broadinstitute.org/gsea/msig	0.06410079	2.78E-05	0
GRAHAM_CML_DIVIDING_VS_NORMAL_QUIESCENT_UP	http://www.broadinstitute.org/gsea/msig	0.08075432	0	0.001056271
REACTOME_CYCLIN_E_ASSOCIATED_EVENTS_DURING_G1_S_TRANSITION_	http://www.broadinstitute.org/gsea/msig	0.08450879	0.021575017	0.024069246
BENPORATH_PROLIFERATION	http://www.broadinstitute.org/gsea/msig	0.0936338	0	0.001335144
GRAHAM_NORMAL_QUIESCENT_VS_NORMAL_DIVIDING_DN	http://www.broadinstitute.org/gsea/msig	0.10780007	0	0
REACTOME_CDK_MEDIATED_PHOSPHORYLATION_AND_REMOVAL_OF_CD	http://www.broadinstitute.org/gsea/msig	0.11104746	0.006053393	0.001100282
SGCGSSAAA_V$E2F1DP2_01	http://www.broadinstitute.org/gsea/msig	0.1132266	0.000446	0.36994377
REACTOME_REGULATION_OF_MITOTIC_CELL_CYCLE	http://www.broadinstitute.org/gsea/msig	0.12175222	0.030714292	0.00874929
REACTOME_E2F_MEDIATED_REGULATION_OF_DNA_REPLICATION	http://www.broadinstitute.org/gsea/msig	0.122322574	2.74E-05	0.01285284
REACTOME_APC_C_CDH1_MEDIATED_DEGRADATION_OF_CDC20_AND_OT	http://www.broadinstitute.org/gsea/msig	0.12268792	0.041439086	0.001123692
REACTOME_APC_C_CDC20_MEDIATED_DEGRADATION_OF_MITOTIC_PROT	http://www.broadinstitute.org/gsea/msig	0.124558374	0.05772412	0.00103512
V$E2F1_Q6	http://www.broadinstitute.org/gsea/msig	0.1419023	8.25E-05	0.21755916
REN_BOUND_BY_E2F	http://www.broadinstitute.org/gsea/msig	0.15824887	0	0.000168
V$E2F1DP2_01	http://www.broadinstitute.org/gsea/msig	0.1583431	0.000641	0.36111528
V$E2F4DP2_01	http://www.broadinstitute.org/gsea/msig	0.15922602	0.000316	0.308822
E2F1_UP.V1_UP	http://www.broadinstitute.org/gsea/msig	0.16001372	0.07726121	0.13206807
V$E2F1DP1_01	http://www.broadinstitute.org/gsea/msig	0.1625169	0.000331	0.3450875
V$E2F1_Q6_01	http://www.broadinstitute.org/gsea/msig	0.1640632	0.004975112	0.37715355
V$E2F_02	http://www.broadinstitute.org/gsea/msig	0.16427012	0.000364	0.30976173
ISHIDA_E2F_TARGETS	http://www.broadinstitute.org/gsea/msig	0.16454798	0	0
REACTOME_ACTIVATION_OF_THE_PRE_REPLICATIVE_COMPLEX	http://www.broadinstitute.org/gsea/msig	0.17069401	0	0.003772688
REACTOME_CELL_CYCLE_MITOTIC	http://www.broadinstitute.org/gsea/msig	0.18161228	0.001131917	0.024216514
V$E2F4DP1_01	http://www.broadinstitute.org/gsea/msig	0.18244343	0.000679	0.3290016
V$E2F1_Q3	http://www.broadinstitute.org/gsea/msig	0.1880097	0.007132111	0.5434143
V$E2F_Q4	http://www.broadinstitute.org/gsea/msig	0.18903509	0.000138	0.39689186
ZHOU_CELL_CYCLE_GENES_IN_IR_RESPONSE_24HR	http://www.broadinstitute.org/gsea/msig	0.19078194	0.008684116	0.002806893
REACTOME_G2_M_CHECKPOINTS	http://www.broadinstitute.org/gsea/msig	0.19329703	0	0.001109398
V$E2F_Q6	http://www.broadinstitute.org/gsea/msig	0.19384018	0.000136	0.3449235
WHITFIELD_CELL_CYCLE_LITERATURE	http://www.broadinstitute.org/gsea/msig	0.20452549	7.48E-05	0.003301728
REACTOME_G1_S_SPECIFIC_TRANSCRIPTION	http://www.broadinstitute.org/gsea/msig	0.20503585	6.67E-05	0.030643823
CHANG_CYCLING_GENES	http://www.broadinstitute.org/gsea/msig	0.21735805	0	0.000558
KEGG_DNA_REPLICATION	http://www.broadinstitute.org/gsea/msig	0.21759363	0	0.116667396
REACTOME_DNA_STRAND_ELONGATION	http://www.broadinstitute.org/gsea/msig	0.2220706	0	0.046146147
REACTOME_MITOTIC_G1_G1_S_PHASES	http://www.broadinstitute.org/gsea/msig	0.23380828	0	0.001282028
KONG_E2F3_TARGETS	http://www.broadinstitute.org/gsea/msig	0.23829126	0	0.000138
OLSSON_E2F3_TARGETS_DN	http://www.broadinstitute.org/gsea/msig	0.25124517	0.18841921	0.3222239
KAUFFMANN_DNA_REPLICATION_GENES	http://www.broadinstitute.org/gsea/msig	0.25620678	0	0.059563834
Cell growth				
REACTOME_MRNA_PROCESSING	http://www.broadinstitute.org/gsea/msig	0.012915834	0.002623442	0.001638745
BURTON_ADIPOGENESIS_PEAK_AT_16HR	http://www.broadinstitute.org/gsea/msig	0.035835117	0	0.08533237
REACTOME_TRNA_AMINOACYLATION	http://www.broadinstitute.org/gsea/msig	0.046439897	0.1984875	0.004750761
RNA_PROCESSING	http://www.broadinstitute.org/gsea/msig	0.04649598	0.001356013	0.011267367
KEGG_SPLICEOSOME	http://www.broadinstitute.org/gsea/msig	0.057477616	0.057894554	0.13498631
REACTOME_REGULATION_OF_ORNITHINE_DECARBOXYLASE_ODC	http://www.broadinstitute.org/gsea/msig	0.06119907	0.028434383	0.005405107
KEGG_AMINOACYL_TRNA_BIOSYNTHESIS	http://www.broadinstitute.org/gsea/msig	0.06144109	0.25855023	0.013828301
MRNA_PROCESSING_GO_0006397	http://www.broadinstitute.org/gsea/msig	0.08926187	0.011572194	0.012224521
REACTOME_TRANSCRIPTION	http://www.broadinstitute.org/gsea/msig	0.09406843	0	0.007614609
REACTOME_RNA_POL_II_TRANSCRIPTION	http://www.broadinstitute.org/gsea/msig	0.10483025	0.059167907	0.012420549
RNA_SPLICINGVIA_TRANSESTERIFICATION_REACTIONS	http://www.broadinstitute.org/gsea/msig	0.19831508	0.11179424	0.21043202
RNA_HELICASE_ACTIVITY	http://www.broadinstitute.org/gsea/msig	0.2004283	0.042425722	0.08311879
REACTOME_MRNA_SPLICING_MINOR_PATHWAY	http://www.broadinstitute.org/gsea/msig	0.20327862	0.028316427	0.017792491
REACTOME_RNA_POL_I_RNA_POL_III_AND_MITOCHONDRIAL_TRANSCRIP	http://www.broadinstitute.org/gsea/msig	0.23740312	0	0.04974437
REACTOME_TRANSPORT_OF_MATURE_MRNA_DERIVED_FROM_AN_INTRC	http://www.broadinstitute.org/gsea/msig	0.24279736	0.049280223	0.04197069
REACTOME_TRANSPORT_OF_RIBONUCLEOPROTEINS_INTO_THE_HOST_NU	http://www.broadinstitute.org/gsea/msig	0.26221517	0.052539285	0.04193959
SPLICEOSOME	http://www.broadinstitute.org/gsea/msig	0.2729094	0.22319931	0.052454144
REACTOME_PROCESSING_OF_CAPPED_INTRONLESS_PRE_MRNA	http://www.broadinstitute.org/gsea/msig	0.27634937	0.23457132	0.042890634
RNA_POLYMERASE_ACTIVITY	http://www.broadinstitute.org/gsea/msig	0.28282723	0.023127701	0.044442423
Cancer/metastasis				
GRADE_COLON_AND_RECTAL_CANCER_UP	http://www.broadinstitute.org/gsea/msig	0.02838891	0.21228471	0.003991324
KOBAYASHI_EGFR_SIGNALING_24HR_DN	http://www.broadinstitute.org/gsea/msig	0.0050721	0	0.000573
SCHLOSSER_MYC_TARGETS_REPRESSED_BY_SERUM	http://www.broadinstitute.org/gsea/msig	0.030234784	0.021466859	0
SOTIRIOU_BREAST_CANCER_GRADE_1_VS_3_UP	http://www.broadinstitute.org/gsea/msig	0.033990975	0	0
BOYAULT_LIVER_CANCER_SUBCLASS_G3_UP	http://www.broadinstitute.org/gsea/msig	0.043235235	0.004435256	0.018923517
NAKAMURA_CANCER_MICROENVIRONMENT_DN	http://www.broadinstitute.org/gsea/msig	0.046736367	0.000668	0.15767501
SARRIO_EPITHELIAL_MESENCHYMAL_TRANSITION_UP	http://www.broadinstitute.org/gsea/msig	0.06540228	0	0.031196702
WINNEPENNINCKX_MELANOMA_METASTASIS_UP	http://www.broadinstitute.org/gsea/msig	0.0807091	0.000266	0.001537526
RHODES_UNDIFFERENTIATED_CANCER	http://www.broadinstitute.org/gsea/msig	0.10512301	0.001352914	0.00111937
KAUFFMANN_MELANOMA_RELAPSE_UP	http://www.broadinstitute.org/gsea/msig	0.105220415	0	0.007739451
TOMIDA_METASTASIS_UP	http://www.broadinstitute.org/gsea/msig	0.10571032	0.041445088	0.21375494
VECCHI_GASTRIC_CANCER_EARLY_UP	http://www.broadinstitute.org/gsea/msig	0.2073714	0.020382322	0.05325398
ODONNELL_TARGETS_OF_MYC_AND_TFRC_DN	http://www.broadinstitute.org/gsea/msig	0.26682377	0.001433474	0.028167572
CROONQUIST_NRAS_SIGNALING_DN	http://www.broadinstitute.org/gsea/msig	0.23664127	0	0.000191
DANG_MYC_TARGETS_UP	http://www.broadinstitute.org/gsea/msig	0.22925662	0.16562039	0
BORCZUK_MALIGNANT_MESOTHELIOMA_UP	http://www.broadinstitute.org/gsea/msig	0.2360386	0.25912035	0.17807612
RHODES_CANCER_META_SIGNATURE	http://www.broadinstitute.org/gsea/msig	0.22573492	0.15227412	0.024029912
DANG_MYC_TARGETS_UP	http://www.broadinstitute.org/gsea/msig	0.22925662	0.16562039	0
BOYAULT_LIVER_CANCER_SUBCLASS_G123_UP	http://www.broadinstitute.org/gsea/msig	0.23370321	0.08395546	0.049637258
SHEDDEN_LUNG_CANCER_POOR_SURVIVAL_A6	http://www.broadinstitute.org/gsea/msig	0.23377588	0.000135	0.01669378
PUJANA_BREAST_CANCER_LIT_INT_NETWORK	http://www.broadinstitute.org/gsea/msig	0.27237272	0.003610279	0.024503974
DAIRKEE_CANCER_PRONE_RESPONSE_BPA	http://www.broadinstitute.org/gsea/msig	0.2751443	0.22182393	0.052520353
SMID_BREAST_CANCER_LUMINAL_A_DN	http://www.broadinstitute.org/gsea/msig	0.29719597	0.020338075	0.003284015

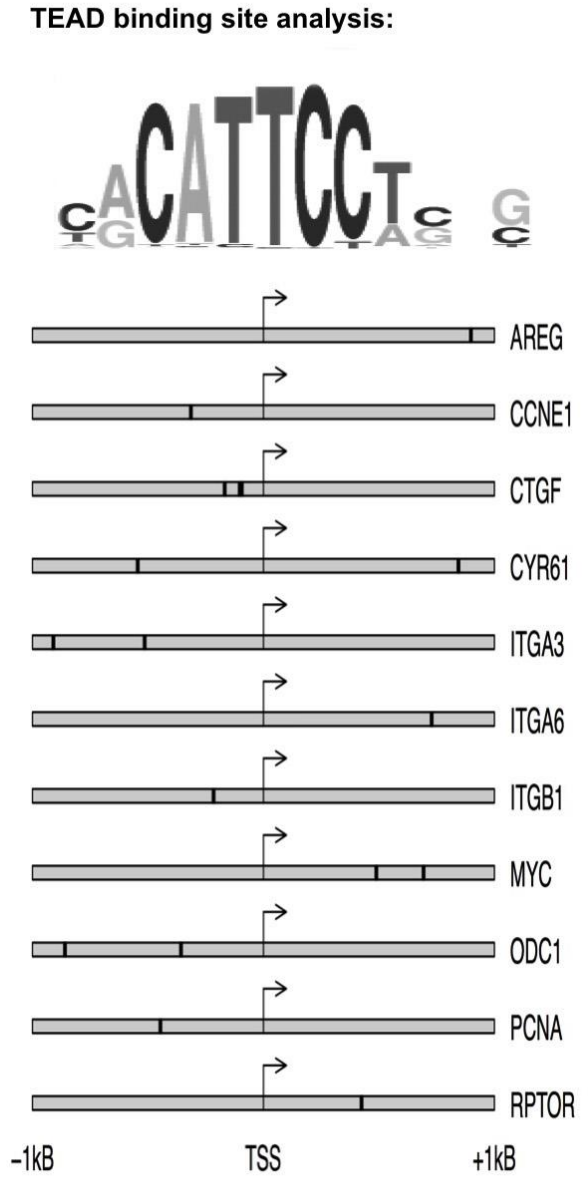

Fig. S1. Gene set enrichment analysis of YAP target genes in keratinocytes. RNAseq analysis was performed on A431 keratinocytes transfected with YAP5SA or siRNA against YAP. Results were compared to HaCaT keratinocytes. Gene sets induced upon YAP5SA expression and decreased upon YAP siRNA are listed in the table. Individual genes that are crucial regulators of each gene set contain several TEAD-specific binding motifs within 1kb of their transcription start sites.

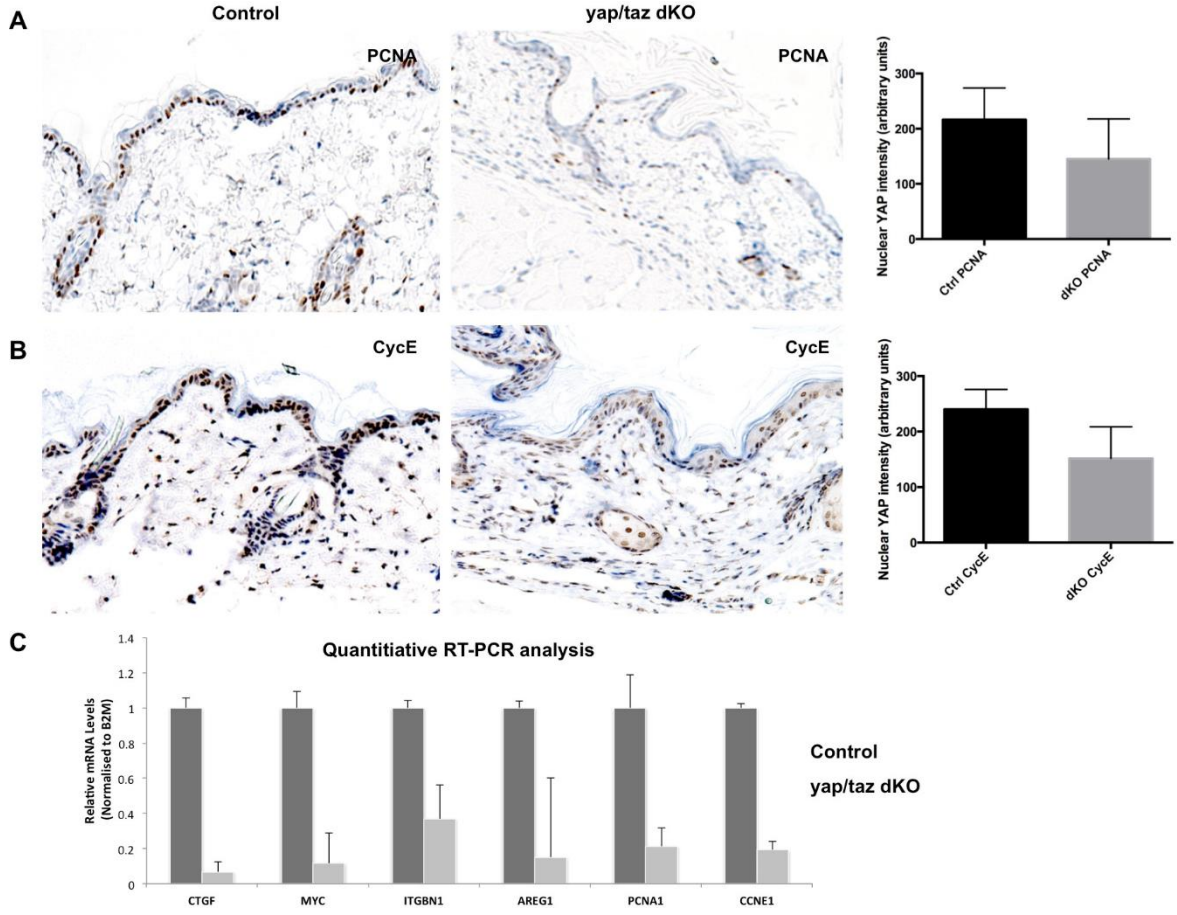

Fig. S2. Reduction in YAP/TAZ target gene expression in yap/taz double knockout skin. Several YAP-dependent genes identified in RNAseq experiments were selected for analysis in wild type versus yap/taz double conditional knockout skin. (A) We find downregulation of PCNA at the protein level by immunostaining. Quantitation was performed on *n*=300 cells from at least 3 different mice. (B) We find downregulation of CyclinE at the protein level by immunostaining. Quantitation was performed on *n*=300 cells from at least 3 different mice. (C) We find downregulation of multiple YAP-dependent genes at the mRNA level by quantitative RT-PCR.

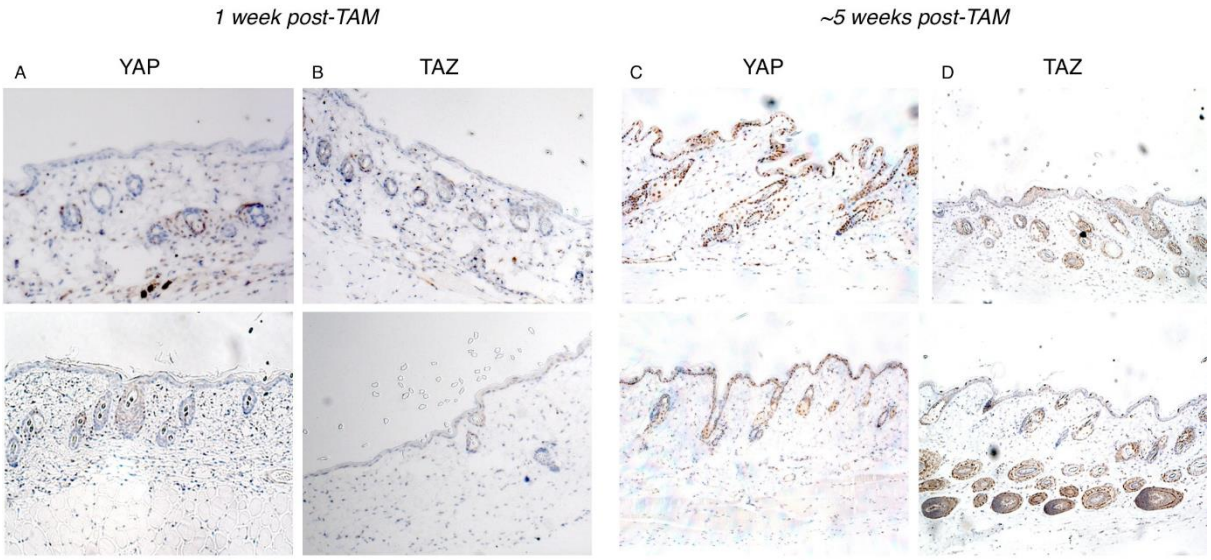

Fig. S3. Repopulation of YAP/TAZ dKO skin by cells escaping Cre-mediated recombination. (A) YAP staining is low in backskin 1 week post-tamoxifen administration (note mosaic deletion). (B) TAZ staining is low in backskin 1 week post-tamoxifen administration. (C) YAP staining is increased in the basal cells of the epidermis, similar to wild type levels, in backskin ~5 week post-tamoxifen administration. (D) TAZ staining is increased in the basal cells of the epidermis, similar to wild type levels, in backskin ~5 week post-tamoxifen administration.

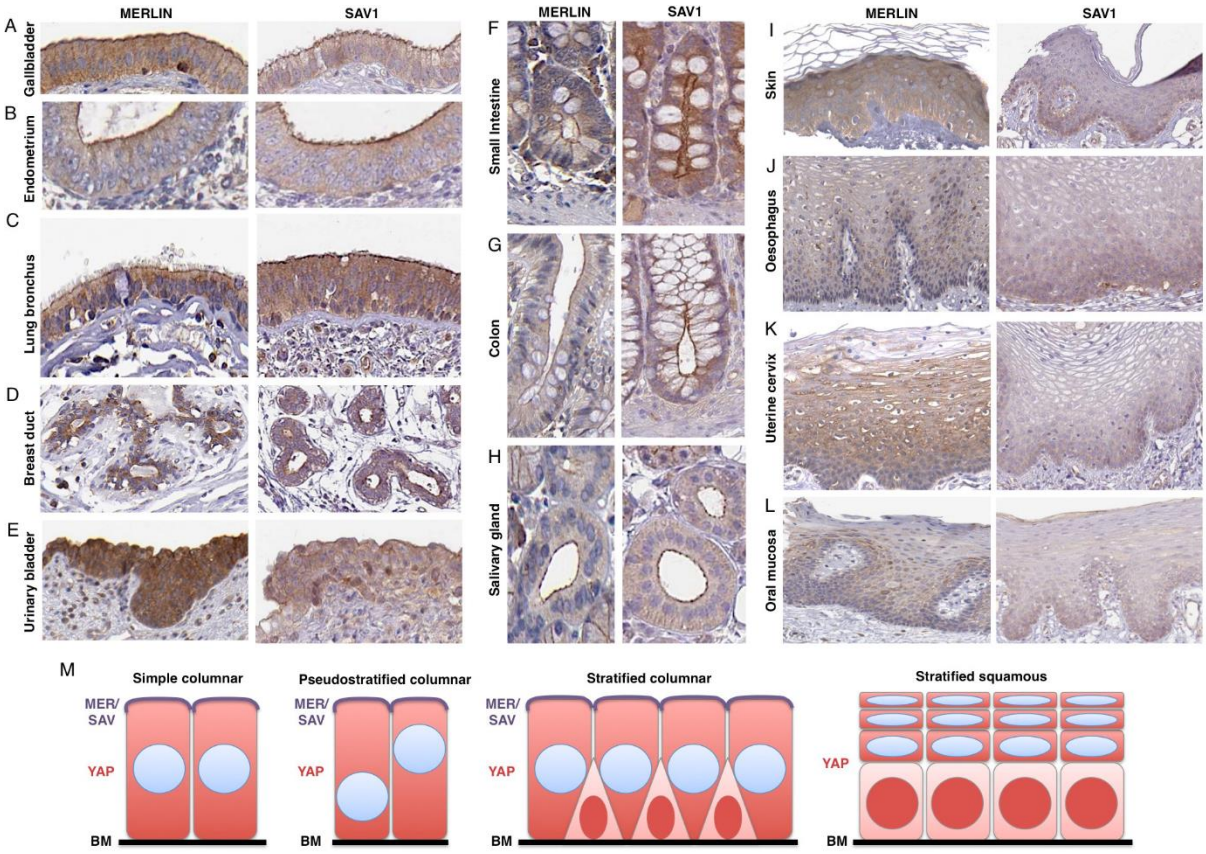

Fig. S4. Merlin and Sav localise in the same manner as Crb3. (A-L) MERLIN and SAV1 localise in the same apical manner as CRB3 in columnar cells of various epithelia. Compare with Fig 3. (M) Schematic diagram of MER/SAV localisation in various epithelial types.

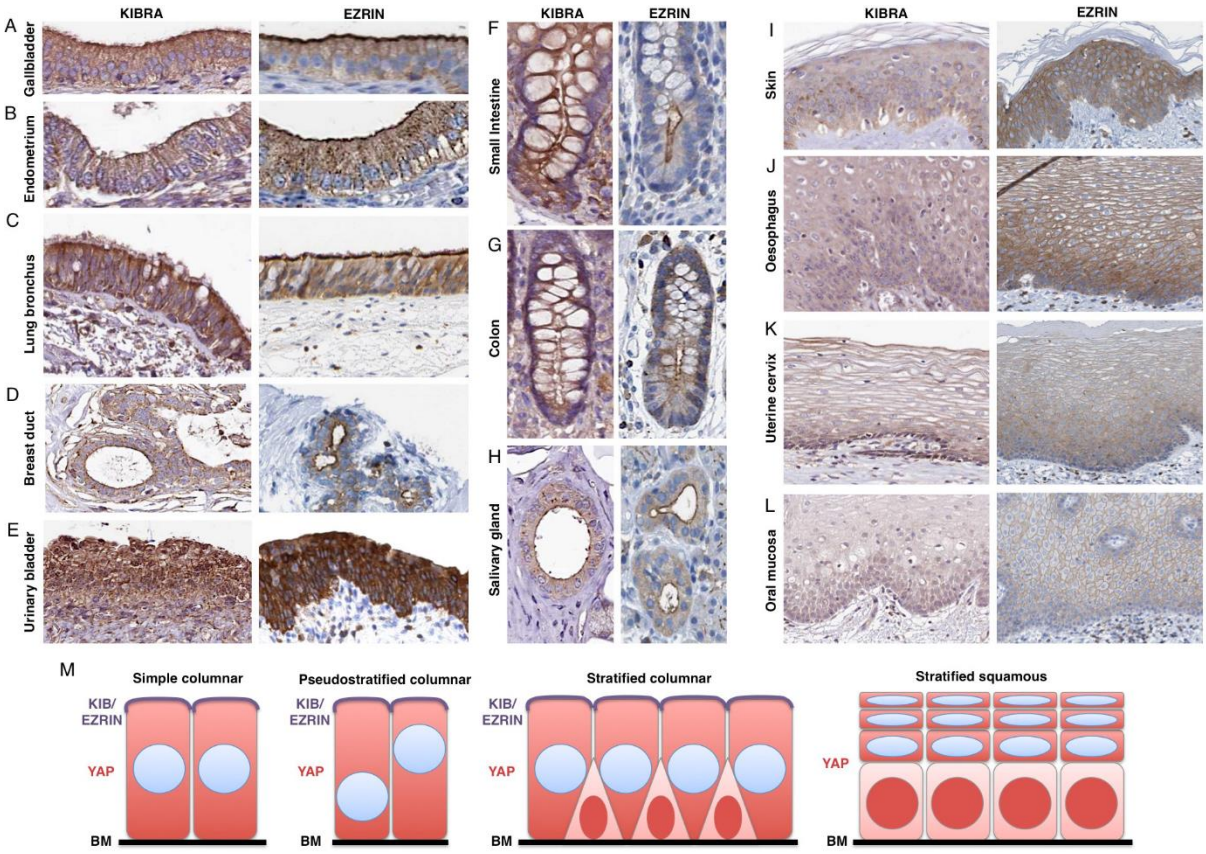

Fig. S5. Kibra and Ezrin localise in the same manner as Crb3. (A-L) KIB and EZR localise in the same apical manner as CRB3 in columnar cells of various epithelia. Compare with Fig 3. (M) Schematic diagram of KIB/EZR localisation in various epithelial types.

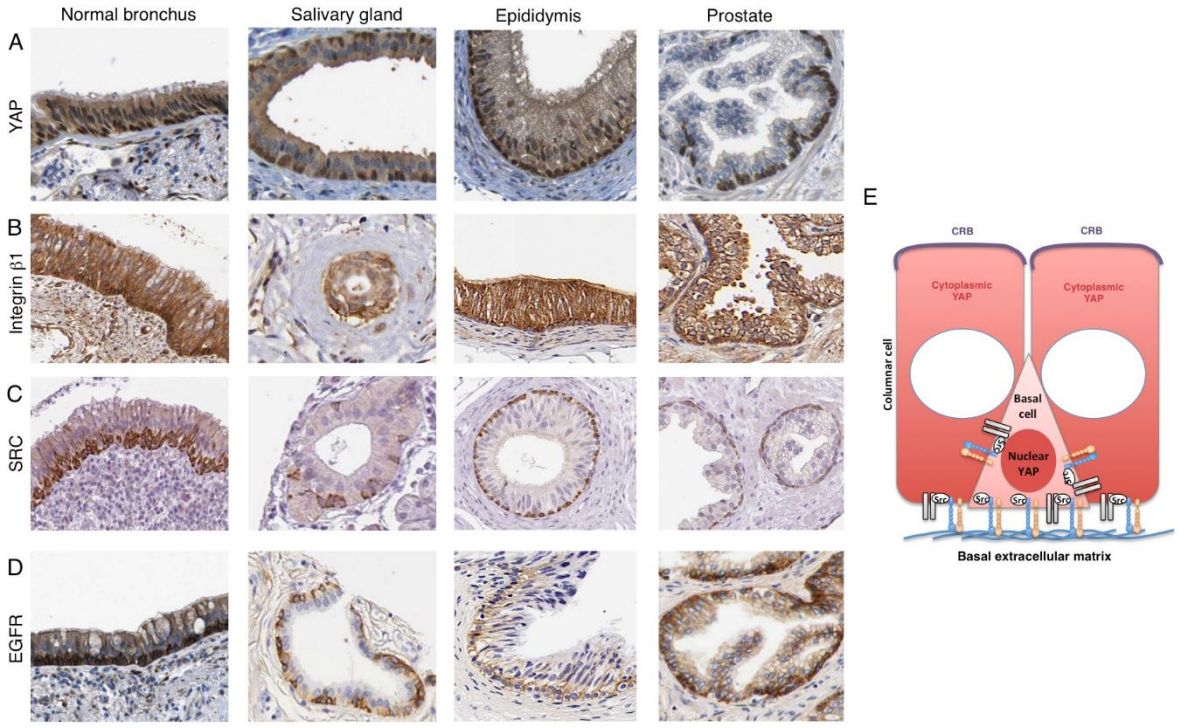

Fig. S6. Integrin-Src-EGFR-YAP localisation in stratified columnar epithelia. Human Protein Atlas data were mined to examine the localisation and expression of YAP, ITGB1, SRC and EGFR. (A) YAP localises to the nucleus in basal layer stem/progenitor cells of bronchus, salivary gland, epididymis and prostate. (B) ITGB1 is expressed in the basal layer stem/progenitor cells of bronchus, salivary gland, epididymis and prostate. (C) SRC is expressed in the basal layer stem/progenitor cells of bronchus, salivary gland, epididymis and prostate. (D) EGFR is expressed in the basal layer stem/progenitor cells of bronchus, salivary gland, epididymis and prostate. (E) Schematic diagram of YAP regulation in stratified columnar epithelia.

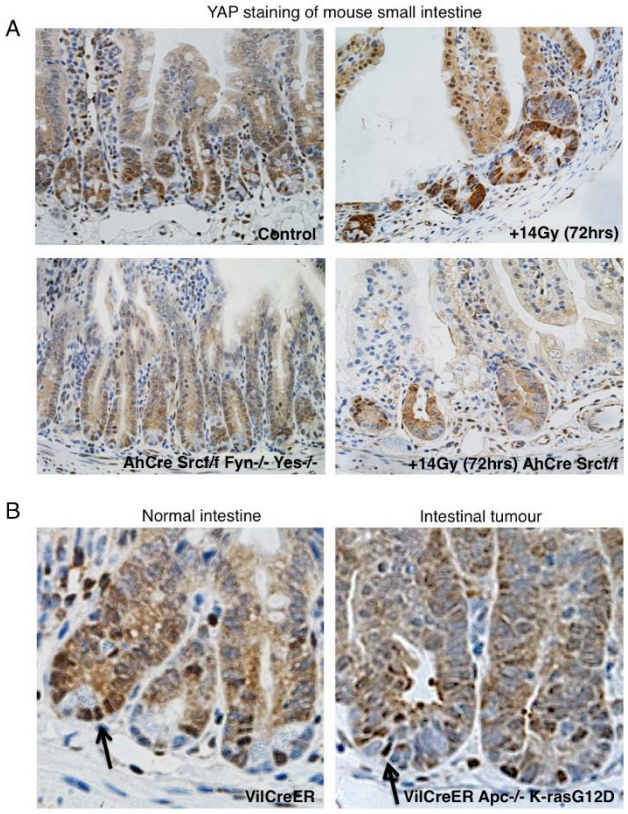

Fig. S7. Src is required for YAP activation after intestinal irradiation. (A) Mouse small intestines stained for YAP before and after 72hrs of gamma-irradiation with 14Gy. Note elevation of YAP levels in crypt progenitor cells. Note decreased YAP levels and nuclear localisation in Src, Fyn, Yes triple knockout intestines or in Src single knockout intestines after 14Gy irradiation. (B) Mouse small intestines from control (Villin-CreER) and Apc K-RasG12D intestines featuring hyperproliferative crypt progenitor expansion. Note that only basal crypt cells feature nuclear YAP, while columnar epithelial cells feature mostly cytoplasmic YAP localisation. Thus, loss of Apc or gain of Ras signalling is not sufficient to induce YAP nuclear localisation *in vivo*.

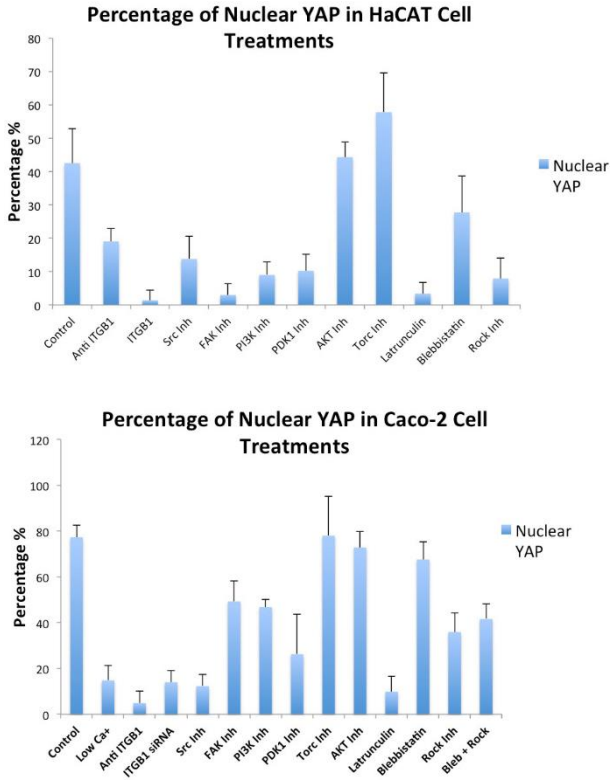

Fig. S8. Comparison of YAP perturbation in HaCAT and Caco-2 cells. Data from Fig 4E and 7G are reproduced to enable direct comparison.